


RESEARCH ARTICLE

Magnitude and Mechanism of Phrenic Long-term Facilitation Shift Between Daily Rest Versus Active Phase

Alexandria B. Marciante , Yasin B. Seven[†], Mia N. Kelly, Raphael R. Perim[‡], Gordon S. Mitchell*

Breathing Research and Therapeutics Center, Department of Physical Therapy and McKnight Brain Institute, University of Florida, Gainesville, FL 32610, USA

* Address correspondence to G.S.M. (e-mail: gsmitche@php.ufl.edu)

[†]Present Address: Department of Physiological Sciences, College of Veterinary Medicine, University of Florida, Gainesville, FL 32610, USA

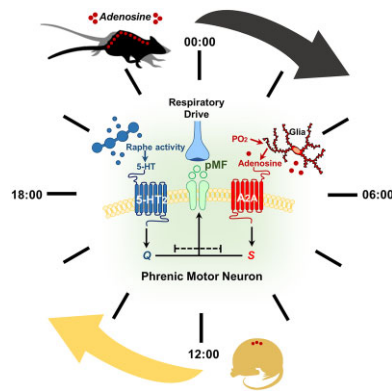
[‡]Present Address: Department of Cellular and Integrative Physiology, University of Texas Health-San Antonio, San Antonio, TX 78229, USA

Abstract

Plasticity is a fundamental property of the neural system controlling breathing. One key example of respiratory motor plasticity is phrenic long-term facilitation (pLTF), a persistent increase in phrenic nerve activity elicited by acute intermittent hypoxia (AIH). pLTF can arise from distinct cell signaling cascades initiated by serotonin versus adenosine receptor activation, respectively, and interact via powerful cross-talk inhibition. Here, we demonstrate that the daily rest/active phase and the duration of hypoxic episodes within an AIH protocol have profound impact on the magnitude and mechanism of pLTF due to shifts in serotonin/adenosine balance. Using the historical “standard” AIH protocol (3, 5-min moderate hypoxic episodes), we demonstrate that pLTF magnitude is unaffected by exposure in the midactive versus midrest phase, yet the mechanism driving pLTF shifts from serotonin-dominant (midrest) to adenosine-dominant (midactive). This mechanistic “flip” results from combined influences of hypoxia-evoked adenosine release and daily fluctuations in basal spinal adenosine. Since AIH evokes less adenosine with shorter (15, 1-min) hypoxic episodes, midrest pLTF is amplified due to diminished adenosine constraint on serotonin-driven plasticity; in contrast, elevated background adenosine during the midactive phase suppresses serotonin-dominant pLTF. These findings demonstrate the importance of the serotonin/adenosine balance in regulating the amplitude and mechanism of AIH-induced pLTF. Since AIH is emerging as a promising therapeutic modality to restore respiratory and nonrespiratory movements in people with spinal cord injury or ALS, knowledge of how time-of-day and hypoxic episode duration impact the serotonin/adenosine balance and the magnitude and mechanism of pLTF has profound biological, experimental, and translational implications.

Submitted: 13 June 2023; Revised: 26 July 2023; Accepted: 27 July 2023

© The Author(s) 2023. Published by Oxford University Press on behalf of American Physiological Society. This is an Open Access article distributed under the terms of the Creative Commons Attribution-NonCommercial License (<https://creativecommons.org/licenses/by-nc/4.0/>), which permits non-commercial re-use, distribution, and reproduction in any medium, provided the original work is properly cited. For commercial re-use, please contact journals.permissions@oup.com



Key words: phrenic long-term facilitation; adenosine; phrenic motor plasticity; daily rest/active cycle

Introduction

Plasticity is a fundamental property of neural systems, including the neural system controlling breathing.¹ Since inspiratory phrenic nerve activity is an “electrical surrogate” of diaphragm muscle activation and respiratory motor output, integrated phrenic nerve activity is often used in studies of respiratory motor plasticity. One important form of phrenic motor plasticity is phrenic long-term facilitation (pLTF) following repeated exposure to brief episodes of low oxygen, or acute intermittent hypoxia (AIH).^{2,3} AIH also elicits plasticity in other respiratory (eg, inspiratory intercostal, hypoglossal, and laryngeal) and non-respiratory motor systems (eg, hand/arm and leg/walking).^{2,4} Beyond its physiological relevance, repetitive AIH is emerging as a promising therapeutic modality to improve breathing, walking, and arm/hand function in people with chronic spinal cord injury^{1,5,6} or ALS.⁷ Greater understanding concerning mechanisms of AIH-induced motor plasticity is essential to optimize its therapeutic benefits.⁴

Phrenic LTF is a persistent increase in phrenic nerve activity lasting hours after episodic electrical stimulation of carotid chemo-afferent neurons^{8–10} or 3, 5 min moderate hypoxic episodes.^{9,11,3} With chemo-afferent neuron stimulation¹² or moderate AIH (mAIH; arterial $PO_2 = 40\text{--}55$ mmHg),¹³ pLTF is driven by a mechanism that requires cervical spinal Gq protein-coupled serotonin 2 (5-HT₂) receptor activation (the “Q pathway”).^{14,15} Conversely, with AIH consisting of severe hypoxic episodes (arterial $PO_2 = 25\text{--}30$ mmHg), pLTF arises from a distinct mechanism that requires cervical spinal Gs protein-coupled adenosine 2A (A_{2A}) receptor activation (the “S pathway”).^{16,17} Serotonin versus adenosine-induced pLTF arise from completely distinct intracellular signaling cascades that interact via powerful crosstalk inhibition^{2,18} (Figure 1). The power of this crosstalk inhibition is demonstrated by the fact that plasticity is abolished when serotonin and adenosine-dependent mechanisms are activated equally by: (1) hypoxic episodes of intermediate severity (arterial $PO_2 = 30\text{--}35$ mmHg)¹⁹; (2) sustained moderate hypoxia²⁰; or (3) concurrent pharmacological activation of both receptor systems.² Thus, the balance of serotonin versus adenosine receptor activation is a powerful regulator of phrenic motor plasticity, and must be considered in experimental design or AIH translation as a therapeutic modality.²

AIH protocols routinely used in rodents (3, 5 min episodes) differ from those most often used in humans (15, 1 min episodes), a difference that may impact pLTF expression. Moderate AIH-induced pLTF requires brainstem raphe neuron activation and increased serotonin release near phrenic motor neurons.¹⁴ On the other hand, spinal tissue hypoxia triggers

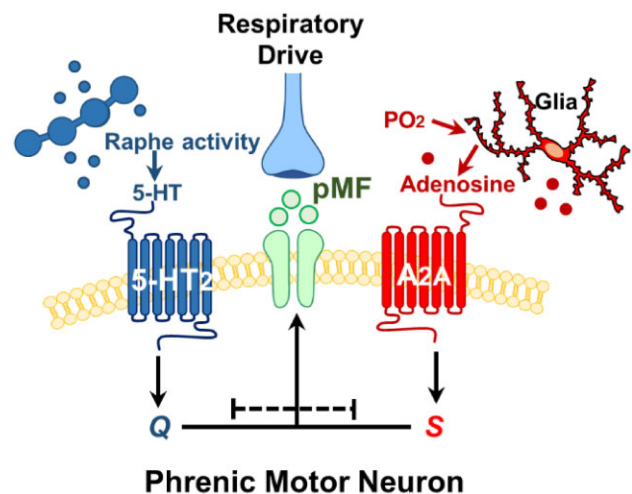


Figure 1. Competing serotonin and adenosine-dependent pathways to phrenic motor facilitation (pMF) interact via powerful crosstalk inhibition. With mAIH, carotid chemoreceptors are stimulated, increasing breathing and (indirectly) brainstem raphe serotonergic neuron activity. Serotonin release in the phrenic motor nucleus initiates the Q pathway to pMF (blue). However, mAIH also elicits spinal tissue hypoxia, triggering glial ATP release and extracellular adenosine accumulation, which undermines serotonin-dominant plasticity due to adenosine 2A (A_{2A}) receptor activation on phrenic motor neurons (ie, S pathway; red). Time of day and hypoxic episode duration effects on pLTF and its underlying mechanism(s) are unknown.

glial ATP release, which is converted to adenosine by extracellular ectonucleotidases.^{2,21,22} Thus, hypoxia-evoked adenosine release and the serotonin/adenosine balance may depend on the severity and duration of hypoxic episodes within AIH protocols.^{16,20} With 3, 5 min mAIH episodes delivered during the rest phase, sufficient spinal adenosine accumulates to attenuate, but not dominate serotonin-driven pLTF.^{18,23,24} The same AIH protocol with severe hypoxic episodes evokes greater spinal adenosine release, shifting the balance to adenosine-dominant pLTF (which is attenuated by serotonin).^{16,25,26} Because the relative activation of these competing cellular mechanisms powerfully regulates AIH-induced pLTF, hypoxic episode duration within AIH protocols likely affects the magnitude or even the dominant mechanism to plasticity.

Another factor that impacts central nervous system (CNS) adenosine levels is the sleep/wake cycle and, presumably, the daily rest versus active phase. CNS adenosine levels increase during wakefulness (particularly in the active phase), thereby increasing “sleep pressure.”^{27–29} Conversely, adenosine levels decrease during sleep (primarily rest phase),^{27,28,30} potentially

minimizing adenosine effects on serotonin-driven phrenic motor plasticity. It has not yet been verified that adenosine concentration exhibits daily fluctuations in the spinal cord. Since studies of AIH-induced respiratory motor plasticity are typically performed during the day—the rest phase in rodents^{2,3} but the active phase in humans^{31,32}—it is crucial to understand time-of-day effects on spinal adenosine levels and AIH-induced respiratory motor plasticity.

The primary goals of this study were to test the hypotheses that: (1) short (1 min) versus longer (5 min) hypoxic episodes evoke less adenosine release despite similar tissue PO₂ levels; (2) AIH consisting of short (1 min) versus longer (5 min) episodes amplifies serotonin-dependent pLTF during the rest phase; (3) background spinal adenosine increases in the midactive phase (versus midrest); and (4) increased adenosine levels during the active phase affect the magnitude and even dominant mechanism of pLTF due to shifts in the serotonin/adenosine balance. We determined the impact of 2 AIH protocols delivered during the midrest versus midactive phase of the day on pLTF: 3, 5 min versus 15, 1 min hypoxic episodes. Although observed changes could arise from the “circadian clock,”³¹ our focus on the rest versus active phase was based on its importance in comparing the outcomes of studies from rodent models versus humans (ie, phase-reversed). Here, we used a urethane-anesthetized rat preparation because of its major advantages in controlling experimental variables (eg, arterial blood gases), its minimal impact on daily rhythms (see the “Discussion” section), and extensive background information available.

We report profound effects of the daily rest/active phase and AIH protocol on the magnitude and even mechanism driving pLTF, and that these effects arise from shifts in the spinal serotonin/adenosine balance. We show that shifts in the serotonin/adenosine balance occur due to the combined effects of: (1) fluctuations in ventral cervical spinal cord adenosine levels across the rest/active cycle; and (2) the duration of hypoxic episodes. During the rest phase, the same cumulative duration of hypoxia presented in shorter hypoxic episodes (15, 1 min versus 3, 5 min hypoxic episodes) nearly doubles pLTF during the rest phase. To our surprise, measurements made during the active phase revealed: (1) attenuated pLTF (versus rest) with the 15 × 1 AIH protocol, but no change in pLTF magnitude following the 3 × 5 AIH protocol; (2) attenuated 15 × 1 AIH-induced pLTF was serotonin-dominant in both phases, but was significantly attenuated in the active phase due to elevated basal adenosine; and (3) pLTF elicited by the conventional 3 × 5 AIH protocol was of similar magnitude in the rest versus active phase, but shifted from a serotonin-dominant (adenosine-constrained) to an adenosine-dominant (serotonin-constrained) mechanism in the active phase.

These findings have profound implications with respect to the design of future experiments, our understanding of mechanisms and functional significance of AIH-induced phrenic motor plasticity, and efforts to harness AIH-induced motor plasticity to treat humans with chronic spinal cord injury or other disorders that compromise breathing or other movements.

Materials and Methods

Animals

All experiments were approved by the University of Florida Institutional Animal Care and Use Committee. Experiments were performed on young (3–4 mo old) male Sprague–Dawley rats (208A Colony, Envigo, IN, USA). Rats were housed in pairs at

24°C with a 12/12 light/dark cycle (lights on at 07:00/lights off at 19:00) and access to food and water *ad libitum*. All rats underwent a 14-d acclimation period prior to use in experiments. Sample size estimation was based on power analysis of previous studies^{15,20,23,33–36} and our extensive experience with this neurophysiological preparation.

Spinal Tissue Sample Collection

Rats were euthanized during midrest (12 PM) and midactive (12 AM) time points. During the midactive phase (12 AM) tissues were collected under a dim red light to minimize light cues. Rats were euthanized under isoflurane anesthesia (4%) via intracardiac perfusion with 1X phosphate-buffered saline (PBS) with a peristaltic pump (Masterflex, Cole-Palmer). Cervical spinal tissue containing the phrenic motor nucleus (C3–C5) was collected and transferred to a microtome (–26°C) to separate ventral from dorsal cervical spinal cord. Tissue was flash frozen in liquid nitrogen and stored at –80°C until use (<3 wk). The mean sample wet weight for ventral C3–C5 spinal cord was: mean (M) = 47.7 mg, SEM = 1.4 mg.

Spinal Adenosine and Serotonin Measurements

Tissue was homogenized in 1X PBS and 200 nM adenosine kinase inhibitor ABT 702 dihydrochloride (Tocris Bioscience) at a concentration of 100 mg tissue/1 mL 1X PBS. Homogenized samples were centrifuged at 10 000 × *g* for 10 min at 4°C. The supernatant was assayed directly.

ADENOSINE ASSAY. The adenosine assay was performed using a coupled enzyme reaction according to methods described by the manufacturer (Cell BioLabs, Inc., REF # MET-5090) but adapted as per Jagermaath et al.³³ Adenosine in ventral C3–C5 or standards is converted to xanthine and hydrogen peroxide through a series of enzymatic reactions. Horseradish peroxidase catalyzes the reaction between hydrogen peroxide and the Oxired probe, binding in a 1:1 ratio. Fluorescence was measured using a FlexStation 3 Multimode Plate Reader (Molecular Devices, San Jose, CA) with excitation at 560 nm and emission at 590 nm. All samples were assayed with and without adenosine deaminase to account for background. The data were analyzed by subtracting fluorescence values from background, and normalizing to protein content. Intra-assay variability was 5.60%.

SEROTONIN ELISA. Spinal C3–C5 serotonin was measured using a rat serotonin ELISA (MyBioSource, REF # MBS166089) according to methods described by the manufacturer. Serotonin in samples binds to a rat serotonin antibody that was precoated on plate wells. Biotinylated rat serotonin antibody binds to sample serotonin, and then bound by Streptavidin-HRP. After incubation, substrate solution is added, and color develops proportionately to the amount of rat serotonin. The reaction is terminated by addition of acidic stop solution and absorbance is measured at 450 nm. Intra-assay variability was 4.66%.

Surgical Preparation

Terminal experiments were performed as previously described.^{16,23,37,38} Rats were induced with 2.5%–3.0% isoflurane in oxygen in a plexiglass chamber, and transferred to a heated surgical table where anesthesia was continued (2.5%–3.0% isoflurane; 60% oxygen, balance nitrogen). Body temperature was monitored with a rectal thermometer (Fisher Scientific, Pittsburgh, PA) and maintained between 37.5°C ± 1.0°C throughout the experiment. A polyethylene catheter (i.d. 1.67 mm; PE

240; Intramedic, MD) was inserted into the trachea through a midline neck incision, and rats were mechanically ventilated (0.07 mL/10 g bw/breath; 72 breaths/min; VentElite small animal ventilator; Harvard Apparatus, Holliston, MA, USA). End-tidal PCO₂ (PETCO₂) was monitored throughout the preparation and experimental protocol using a breath through capnograph with sufficient response time to monitor true end-tidal CO₂ levels in rats (Capnogard, Novamatrix, Wallingford CT). The inspired CO₂ fraction was adjusted as needed to keep end-tidal CO₂ within physiological limits.

Anesthesia was then slowly converted to urethane via slow infusion into a venous into tail vein catheter (1.8 g/kg at 6 mL/h; 24 gauge, Surflo, Elkton, MD), while progressively decreasing inspired isoflurane concentration 0.5% every 6 min. Anesthetic depth was assessed during conversion by lack of response to a toe-pinch; supplemental anesthetic was infused if required. Rats were bilaterally vagotomized at the midcervical level to prevent phrenic nerve entrainment with the ventilator. The right femoral artery was isolated and cannulated with polyethylene tubing (I.D. 0.58 mm; PE 50; Intradermic, MD) to monitor blood pressure (TA-100 Transducer Amplifier, CWE, Inc.) and sample blood gases (PaO₂, PaCO₂ and acid-base balance (pH, base excess, and hemoglobin) with a blood gas analyzer (ABL 90 Flex, Radiometer, Copenhagen, Denmark). Once urethane conversion was complete, intravenous fluids were administered to maintain fluid and acid-base balance (1.5 mL/h; 1:4 of 8.4% Na₂CO₃ in lactated Ringer's solution). Rats were then paralyzed with pancuronium bromide (2 mg/kg; Sigma-Aldrich, St. Louis, MO).

SERIES I: Micro-Optode Measurements for Spinal PtO₂

A dorsal midline incision was made from the base of the skull to the fifth cervical segment. Muscle layers were retracted to expose C3–C5 vertebrae. A laminectomy was performed at the C₄ vertebrae. A longitudinal cut was made in the dura to enable insertion of a 50 μm oxygen micro-optode mounted on a micro-manipulator (Unisense; Aarhus, Denmark). The optical sensor tip was coated with a fluorophore that, when excited with 610 nm red light pulses, emits 780 nm infrared light that varies with an intensity inversely proportional to oxygen partial pressure. The micro-optode was placed on the left side, 1 mm lateral to midline and ~1.5 mm deep to measure PtO₂ near/in the phrenic motor nucleus, as previously described.³⁹ Coordinates were obtained from previous studies.⁴⁰

Raw signals were acquired at 1 Hz and converted to mmHg via two-point calibration. Saline was warmed to 37°C and aerated with 21% oxygen over 40 min for the first calibration point (ie, normoxia). Sodium hydroxide (0.1 M) and sodium ascorbate (0.1 M) were then added in warmed saline to create an anoxic solution for the second calibration point (ie, zero oxygen). Measurements began ~45 min after probe placement. Rats were then exposed to 5 min of 13% O₂ or 1 min of 9% O₂ (n = 4 each group; PaO₂ = 40–50 mmHg). Calibration was verified *in vivo* by observing PtO₂ values of 0–1 mmHg several minutes after a urethane overdose (not shown).

SERIES II: Adenosine and Inosine Probe Measurements for Changes in Spinal Extracellular Adenosine

In separate rats (n = 3) changes in extracellular adenosine concentration (ΔADO) were measured during 5 min of 13% inspired O₂ and 1 min of 9% inspired O₂ (PaO₂ = 40–50 mmHg). Using the same surgical procedures and probe placement described in “SERIES I” experiments, extracellular ΔADO concentrations were measured by differential enzymatic detection using

adenosine and inosine microbiosensors (Zimmer-Peacock, UK) positioned ~1 mm lateral to the spinal midline between C3 and C4 (~1.5 mm depth). Microbiosensors were approximately 3–4 mm apart from each other on the same side of the spinal cord. The signals were acquired at 1 Hz and converted to concentrations using a three-point calibration. Measurements began ~30–45 min after probe insertion. Probe functionality was verified at the end of each experiment.

SERIES III: Neurophysiological Experiments

A laminectomy was performed at the C2 vertebrae for intrathecal drug delivery. A small hole was cut in the dura near the junction of the C2 and C3 segments, and a flexible silicone catheter (O.D. 0.6 mm; Access Technologies) was fed through to the caudal end of C3. A 50 μL Hamilton syringe containing drug (see the “Drugs and Vehicles” section) was attached to the catheter for drug delivery. To prevent off target effects of pharmacological manipulation, we used intrathecal drug injections directly at C4 versus systemic administration to limit unintended drug distribution. For example, in an anatomically separated structure, LTF in hypoglossal (XII) motor output (brainstem structure rostral the phrenic nerve) has been measured simultaneously in previous reports from our lab, and found to be unaffected by intrathecal drug delivery at C4,^{14,23} at least with injection volumes less than 20 μL.

Drugs and Vehicles

Drugs used throughout studies include MSX-3 (A_{2A} receptor antagonist; #M3568; Millipore Sigma), ketanserin tartrate (5-HT_{2A/C} receptor antagonist; #090850; FisherSci), and istradefylline (A_{2A} receptor antagonist; #51470R; FisherSci). Upon arrival, all drugs were dissolved in 100% DMSO or 0.9% saline based on solubility and manufacturer information. Aliquots of these stock solutions were kept frozen at –20°C. On the day of experiments, drugs were diluted in sterile 0.9% saline to achieve the desired final concentration. The final DMSO-saline ratios were determined by drug solubility; a final concentration of 10% DMSO was sufficient to dissolve all drugs in the vehicle solution. Most drugs were dissolved to final effective concentrations previously determined in our laboratory via published dose-response studies.¹⁵ Based on these (and other) reports, intrathecal drug doses were as follows: 10 μM MSX-3 (12 μL),¹⁶ 1 mM istradefylline (12–15 μL), and 500 μM ketanserin tartrate (18 μL).¹⁵

Electrophysiological Recordings

Using a dorsal approach, the left phrenic nerve was isolated, cut distally and de-sheathed. Custom suction recording electrodes filled with 0.9% saline were then placed in the saline-filled phrenic pocket and the nerve was suctioned up with a 60 mL syringe to record respiratory neural activity. Nerve activity was amplified (10 K, A-M systems, Everett, WA), filtered (bandpass 300–5000 Hz), integrated (time constant, 50 ms), digitized (CED 1401, Cambridge Electronic Design, UK), and analyzed using Spike2 software (CED, version 8.20). Inspiratory phrenic activity served as an index of respiratory motor output.

Experimental Protocols

At least 45 min after conversion to urethane anesthesia, CO₂ apneic and recruitment thresholds of phrenic nerve activity were determined by: (1) lowering inspired CO₂ levels, or (2) increasing ventilation rate until rhythmic respiratory

nerve activity ceased. After ~1 min, inspired CO₂ levels were slowly increased until respiratory rhythmic respiratory activity resumed. Baseline conditions were established by raising PETCO₂ ~2 mmHg above the recruitment threshold. Blood samples were taken during baseline to document blood gas levels during stable nerve activity. Arterial PCO₂ was maintained isocapnic (\pm 1.5 mmHg) with respect to baseline blood gas values by actively manipulating inspired CO₂ concentration and/or ventilation rate. Baseline oxygen levels (60% oxygen, balance nitrogen, and carbon dioxide; PaO₂ \geq 150 mmHg) were maintained throughout experiments, except for hypoxic challenges (PaO₂ = 40–55 mmHg). At the end of protocols, a maximum chemoreceptor challenge (7% CO₂, 10% O₂, balance N₂) was administered for ~3 min to ensure preparation stability and adequate dynamic range in phrenic nerve amplitude (data in Supplement). Rats were euthanized by urethane overdose.

Statistical Analyses

Measurements of peak integrated phrenic burst amplitude and burst frequency (bursts/min) were assessed in 1 min bins immediately before each arterial blood sample at: baseline, during last minute of first hypoxic episode (short-term hypoxic response; STHR), 30, 60, and 90 min post-AIH, and during the final minute of the maximum chemoreflex challenge (Table S3). Measurements were made at equivalent time points in time-matched control experiments. Integrated nerve burst amplitude was normalized by subtracting the baseline value, dividing the difference by the baseline value, and reporting percentage changes from baseline. Burst frequencies were also normalized to baseline, expressed as an absolute difference in bursts per minute. All statistical comparisons between treatment groups for nerve burst amplitude (baseline and 90 min) were made using a 2- or 3-way ANOVAs with a repeated measures design. Individual comparisons were made using the Tukey post-hoc test.

Comparisons of mean arterial pressures, arterial PCO₂ and PO₂ (Tables S1 and S2), and burst frequency (Table S4) were made at baseline, during hypoxia episode 1, 30, 60, and 90 min post-AIH using a 2-way ANOVA to determine if there was an effect of time-of-day on baseline values; 2-way mixed effects ANOVA was used to test if there was an effect of protocol with drug pretreatment. Comparisons in spinal adenosine and serotonin levels during midrest versus midactive phases were made with unpaired t-tests. The spinal PtO₂ signal was smoothed and analyzed in 1-min averages before AIH, during the nadir of the first hypoxic episode, and reoxygenation peak following the first hypoxic episode. Unpaired t-tests were used to compare measurements of PtO₂ and Δ ADO during 5 versus 1 min hypoxic episodes (PaO₂ = 40–50 mmHg).

Three-way repeated measure ANOVA and mixed effect ANOVA designs were calculated using JMP Pro (version 16.1.0; SAS Institute, Inc. Cary, NC, USA). All other statistics were analyzed in SigmaPlot (version 14.0.0.124; Systat Software Inc., San Jose, CA, USA). Differences between groups were considered significant if $P < .050$. Data are presented as mean \pm SEM.

Results

Basal Ventral Spinal Adenosine Fluctuates with the Daily Rest/Active Cycle

While adenosine levels fluctuate throughout the daily rest/active cycle in multiple brain regions,^{27,30} it is unknown if the spinal cord exhibits a similar pattern. There is limited

evidence that circadian clock genes oscillate within the phrenic motor system,⁴¹ and time awake increases brain adenosine (regardless of time of day)^{27,30,42}; thus, spinal adenosine may fluctuate across the daily rest/active cycle. To test this hypothesis, ventral cervical segments 3–5, which contain the phrenic motor nucleus, were harvested in the rat midrest (12 PM) and midactive (12 AM) phases to assess adenosine and serotonin levels ($n = 6$ per group). Throughout harvesting, care was taken to minimize light cues^{33,43}; for example, tissues collected in the midactive phase were harvested under transient dim red light. Spinal adenosine was measured with a fluorometric assay (Cell BioLabs; as adapted by Jagannath et al. 2021).³³ Ventral C3–C5 adenosine was significantly higher during the midactive ($14.5 \pm 1.8 \mu\text{M}$) versus midrest phase ($7.1 \pm 1.4 \mu\text{M}$; $t_{10} = 3.099$, $P = .011$; unpaired t-test; Cohen's $d = 2.031$; Figure 2A).

Given the importance of serotonin in AIH-induced pLTF, basal serotonin levels were also measured in the same homogenates using a rat serotonin ELISA (MyBioSource). There was no difference in serotonin between the midrest ($46.6 \pm 3.3 \text{ ng/mL}$) and midactive phase ($46.3 \pm 2.3 \text{ ng/mL}$) ($t_{11} = 0.084$, $P = .935$; unpaired t-test; Cohen's $d = 0.459$; Figure 2B), consistent with a report in the rat lumbar spinal cord.³⁴

We also measured adenosine 2A (A_{2A}) receptor protein levels (Figure S1) in the cervical spinal cord, and found no differences between midrest versus midactive samples. Prior work indicates no difference in ventral spinal 5-HT_{2A} receptor expression at either phase.⁴¹ Thus, whereas ventral cervical spinal adenosine levels fluctuate across daily rest/active phases in spinal regions associated with the phrenic motor nucleus, similar effects do not occur in spinal serotonin concentration or A_{2A} receptor expression.

pLTF Magnitude is the Same at Midrest and Midactive with the “Standard” mAIH Protocol

Moderate AIH (3, 5 min hypoxic episodes, 5 min duration; arterial PO₂ > 40 mmHg) has been used in most published studies of pLTF.⁴ Thus, we recorded phrenic nerve activity in anesthetized, paralyzed, vagotomized, and artificially ventilated rats prepared for phrenic nerve recordings (for details concerning experimental preparation, see refs.^{15,44}). In the midactive phase, care was taken to prevent light cues—rats were prepared for surgery and anesthetized under a dim red light before being transferred to the experimental rig. After transferring rats to the rig, their eyes were immediately covered. Once adequate anesthesia was confirmed by lack of a toe-pinch reflex, room lights were turned on, but their eyes remained covered for the duration of experiments.

Ventilator tidal volume (mL) was set based on body mass ($0.007 \text{ mL} \times \text{body mass, g}$). Ventilator rate was maintained between 72 and 74 breaths per minute. During baseline conditions, rats were ventilated with 60% O₂ (balance N₂). Inspired CO₂ was adjusted to maintain end-tidal PCO₂ between 38 and 41 mmHg since CO₂ influences phrenic nerve activity.^{9,10,13,45,46} To standardize baseline conditions at the beginning of experiments, CO₂ apneic and recruitment thresholds were determined. After establishing the CO₂ recruitment threshold, the arterial carbon dioxide partial pressure (PaCO₂) was raised ~2 mmHg above that threshold; once set, PaCO₂ was actively maintained within \pm 1.5 mmHg throughout the experiment (Table S1). Rectal temperature was measured and maintained at $37.5^\circ\text{C} \pm 1.0^\circ\text{C}$.

The “standard” mAIH protocol consists of 3, 5 min episodes of moderate hypoxia (arterial partial pressure of oxygen, PaO₂:

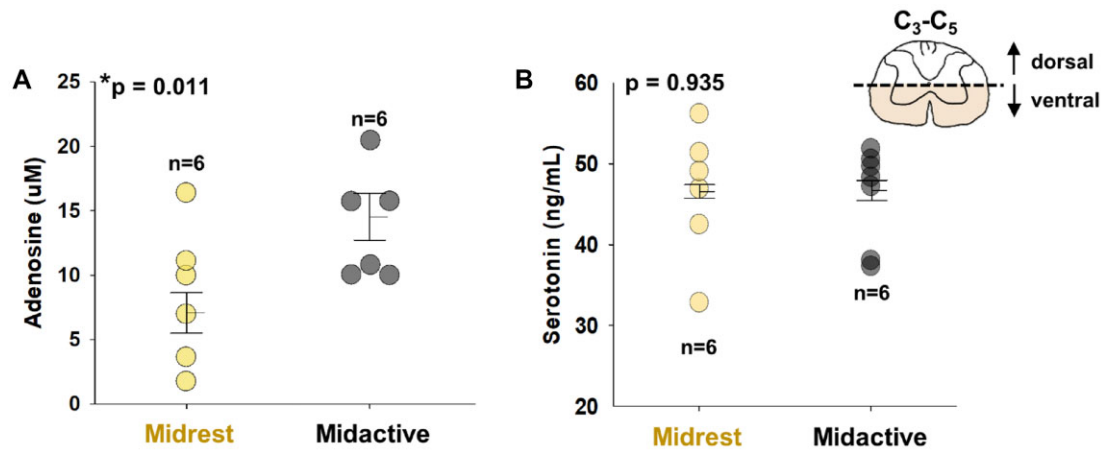


Figure 2. Basal spinal adenosine levels are greater in active versus rest phase. (A) Ventral spinal C3–C5 adenosine concentration is significantly elevated during midactive (midnight; black) versus midrest (noon; yellow) phase ($P = .011$). (B) Basal serotonin levels measured at these same time points are not different ($P = .935$). All groups, $n = 6$; comparisons were made using unpaired t-test. Bars show means ± 1 SEM; $P < .050$.

40–55 mmHg), with 5 min intervals of baseline conditions^{9,11,3} (Figure 3A). Following mAIH, baseline conditions were restored ($\text{PaO}_2 > 150$ mmHg; Figure 3A and B) and actively maintained while phrenic nerve activity was measured for 90 min. Moderate AIH was delivered during midrest (12 PM) or midactive (12 AM) phases of the day. Blood gas measurements were taken 2–3 times to establish the initial baseline, and then at the nadir of hypoxic episodes, and 30, 60, and 90 min post-mAIH (Tables S1 and S2). One-minute averages of integrated phrenic nerve burst amplitude were measured 90 min post-mAIH, and expressed as % change from pre-AIH baseline values. Raw integrated phrenic nerve amplitude at baseline and during maximal chemoreceptor stimulation (10% O_2 , 7% CO_2 , balance N_2) delivered at the end of each experiment are included in Table S3 to assess recording quality. Phrenic burst frequency is shown in Table S4.

We originally hypothesized that serotonin-dependent mAIH-induced pLTF would be lower in the midactive versus midrest phase due to elevated background adenosine levels. However, pLTF magnitude was similar in the midrest ($56.1\% \pm 5.2\%$ pLTF; $n = 7$) versus midactive phase ($50.5\% \pm 4.4\%$ pLTF; $n = 7$; $F_{1,27} = 0.667$, $P = .430$, two-way RM ANOVA; Cohen's $d = 0.436$; Figure 3C–E). Integrated phrenic nerve burst amplitude 90 min post- 3×5 mAIH was significantly elevated versus baseline activity, indicating significant pLTF ($F_{1,12} = 245.994$, $P < .001$, two-way RM ANOVA), during midrest and midactive phases (both $P < .001$; Tukey post-hoc). Since pLTF magnitude was unchanged by rest/active phase despite elevated basal adenosine levels in the active phase, we wondered if the combined time-of-day and 5 min hypoxic episodes effects were sufficient to flip pLTF from serotonin- to adenosine-dominance.

pLTF Elicited by 3, 5 Min Moderate Hypoxic Episodes Shifts Between Serotonin and Adenosine Dominance

To address the possibility that there is a shift in mechanism from Q (serotonin) to S (adenosine) pathway dominance in the midrest versus midactive phase, we tested the hypothesis that cervical spinal A_{2A} receptor inhibition impairs pLTF in the midactive phase, even though it is known to augment mAIH-induced pLTF in the rest phase.²³ Thus, the A_{2A} receptor antagonist, MSX-3 (10 μM , 12 μL), was delivered intrathecally at C4 to localize inhibition near the phrenic motor nucleus^{14,23} 12 min

prior to 3×5 min mAIH to determine if increased adenosine during the midactive phase is sufficient to flip mAIH-induced pLTF from a serotonin- to an adenosine-driven mechanism (Figure 4A).

Although baseline phrenic nerve activity was unaffected by drug administration (Figure S2), 3×5 mAIH elicited significant pLTF; further, rest/active phase and MSX-3 significantly affected pLTF magnitude in the overall ANOVA ($F_{1,24} = 52.27$, $P < .001$, three-way RM ANOVA; Figure 4B and C). However, MSX-3 significantly enhanced 3×5 mAIH-induced pLTF during midrest ($141.4\% \pm 14.8\%$ pLTF; $n = 7$) versus vehicle ($P < .001$, Tukey post-hoc; Cohen's $d = 3.115$) and baseline ($P < .001$, Tukey post-hoc), confirming prior reports.^{16,23} In striking contrast, when 3×5 mAIH plus MSX-3 were delivered in the midactive phase, pLTF was significantly reduced ($19.1\% \pm 7.6\%$ pLTF; $n = 7$) versus 3×5 mAIH alone ($P = .007$, Tukey post-hoc; Cohen's $d = 1.901$; Figure 4B and C). The reverse effects of cervical spinal A_{2A} receptor inhibition on 3×5 mAIH-induced pLTF in the midrest versus midactive phase is consistent with a shift from serotonin-dominant, adenosine constrained (midrest) to an adenosine-dominant, serotonin constrained mechanism (midactive). This mechanistic flip likely arises from the combined effects of elevated basal adenosine levels with hypoxia-induced adenosine release during 5 min episodes delivered in the midactive phase.

To verify this hypothesis, the serotonin 2A/C (5-HT_{2A/C}) receptor antagonist, ketanserin tartrate (500 μM , 18 μL), was delivered intrathecally at C4 to block serotonin-dependent Q pathway activation (Figure 4D). Again, we found significant effects of 3×5 mAIH, rest/active phase, and ketanserin on pLTF magnitude ($F_{1,16} = 29.187$, $P < .001$, three-way RM ANOVA). During midrest, ketanserin ($n = 3$) reduced pLTF to $20.2\% \pm 8.6\%$ ($P = .022$, Tukey post-hoc; Cohen's $d = 2.515$; Figure 4E and F), and was not significantly different from baseline ($P = .680$, Tukey post-hoc), confirming prior reports.¹⁵ Ketanserin had profound effects during the midactive phase, however, and enhanced pLTF ($123\% \pm 27\%$; $n = 3$) versus 3×5 mAIH alone ($P < .001$, Tukey post-hoc; Cohen's $d = 2.126$; Figure 4E and F). Thus, although 3×5 mAIH induces similar pLTF magnitude in the midrest and midactive phase, it does so by entirely different mechanisms, shifting from serotonin-dominant, adenosine constrained at midrest, to adenosine dominant, serotonin constrained in the midactive phase.

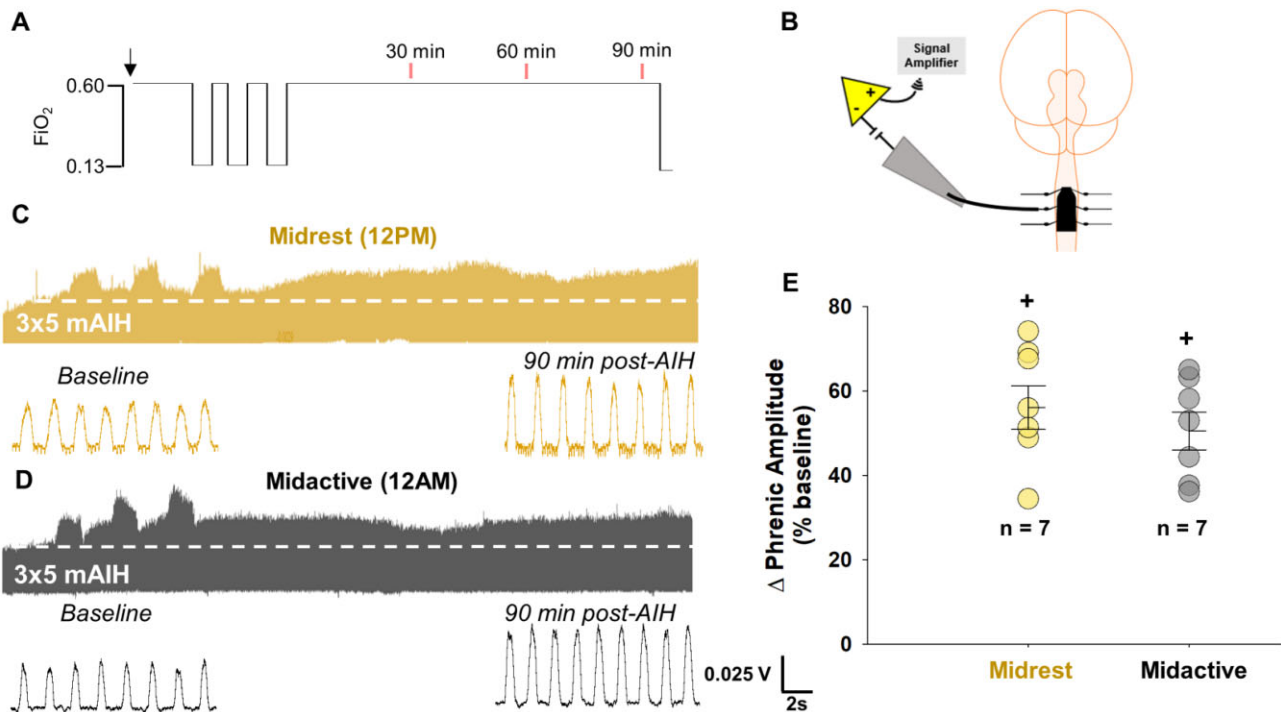


Figure 3. Phrenic LTF elicited by 3×5 mAIH is similar during midrest and midactive phases. 3×5 mAIH was delivered at noon or midnight to rats on a normal light cycle (A). Phrenic nerve activity was recorded in urethane anesthetized rats before, during and after 3×5 mAIH (B). Representative compressed neurogram of integrated phrenic nerve activity during baseline, mAIH (Hx1-3; $\text{PaO}_2 = 40\text{--}55$ mmHg), and for 90 min after restoring baseline conditions during midrest (12 PM; C) and midactive phases (12 AM; D) are shown. Phrenic amplitude as a % change from baseline (% pLTF; E) at 90 min post 3×5 mAIH was not different between the midrest and midactive phases ($n = 7$ each group; $P = .430$; two-way RM ANOVA). Bars show mean \pm SEM. + $P < .001$, significant differences versus baseline. Hx, hypoxia; FIO_2 , fraction of inspired oxygen; mAIH, moderate acute intermittent hypoxia; pLTF, phrenic long-term facilitation.

Shorter Hypoxic Episodes Minimize Evoked Adenosine Release in the Phrenic Motor Nucleus

Hypoxic episodes elicit rapid carotid chemoreceptor and subsequent brainstem serotonergic neuron activation.^{4,3,47} In contrast to the rapid carotid chemoreceptor-driven effects, hypoxia spreads more slowly to spinal cord tissues, where it triggers glial ATP release with subsequent conversion to adenosine. Thus, hypoxia-evoked spinal ATP release and adenosine accumulation is slower than the neural network activation that triggers serotonin release and Q pathway activation. Based on these differences in time course, shorter hypoxic episodes were hypothesized to emphasize serotonergic versus adenosinergic mechanisms of pLTF. Although 5 min hypoxic episodes give adequate time to reach a nadir in spinal tissue hypoxia,³⁹ parsing hypoxia of the same cumulative duration (15 min) into shorter episodes (15×1 min) may minimize tissue hypoxia and hypoxia-evoked adenosine accumulation. Thus, we hypothesized that 5 versus 1 min episodes of the same moderate hypoxia (defined by tissue PO_2) evoke greater adenosine accumulation.

To test this hypothesis, spinal tissue PO_2 was measured using a $50 \mu\text{M}$ optical sensor (Unisense; Aarhus, Denmark) positioned 1 mm lateral to midline between C3 and C4, approximately 1.5 mm below the surface of the spinal cord (Figure 5A; see ref. 39). We presented 1 versus 5 min moderate hypoxic episodes, with the inspired O_2 adjusted to achieve the same tissue PO_2 nadir within episodes. Hypoxia was delivered as: (1) 5 min of 13% inspired O_2 ($\text{PaO}_2 = 46.6 \pm 3.9$ mmHg; Figure 5B); or (2) 1 min at 9% inspired O_2 ($\text{PaO}_2 = 46.2 \pm 1.3$ mmHg; Figure 5C; $n = 4$ per group); the difference in inspired O_2 is not fully reflected in tissue PO_2 since there is insufficient time to reach steady state

during 1 min episodes. In the rats studied, no differences in baseline tissue PO_2 were observed ($t_6 = 0.12$, $P = .912$; unpaired t-test; Figure 5D). Despite differences in inspired oxygen concentration delivered during 5 (13% O_2) versus 1 (9% O_2) min episodes, spinal PtO_2 achieved similar levels: $\text{PtO}_2 = 13.8 \pm 2.8$ mmHg and 12.5 ± 1.2 mmHg for 5 and 1 min hypoxic episodes, respectively ($t_6 = 0.42$, $P = .689$; unpaired t-test; Cohen's $d = 0.600$; Figure 5E). Tissue reoxygenation was similar after 5 and 1 min episodes ($t_6 = -0.44$, $P = .678$; unpaired t-test; Figure 5F).

Hypoxia-evoked adenosine release was measured in the ventral cervical spinal cord near the phrenic motor nucleus via adenosine and inosine microbiosensors (Zimmer-Peacock, UK) during 5 and 1 min hypoxic episodes ($n = 3$ per group; Figure 5G). With 5 min hypoxic episodes, significantly higher peak adenosine levels were observed versus 1 min episodes (5 min: $3.5 \pm 0.1 \mu\text{M}$; 1 min: $2.1 \pm 0.2 \mu\text{M}$; $t_4 = 6.04$, $P = .004$; unpaired t-test; Cohen's $d = 4.933$; Figure 5H). When expressed as the area under the curve to reflect total adenosine accumulation during hypoxic episodes, significantly more adenosine accumulated during 5 versus 1 min episodes (5 min: $17.4 \pm 0.4 \mu\text{M}$; 1 min: $2.1 \pm 0.21 \mu\text{M}$; $t_4 = 33.10$, $P < .001$; unpaired t-test; Cohen's $d = 27.026$; Figures 5I). Thus, shorter hypoxic episodes evoke less spinal adenosine accumulation near phrenic motor neurons, despite attainment of similar arterial and spinal tissue PO_2 levels.

Overall, these data support the idea that adenosine accumulation during 5 min hypoxic episodes, when superimposed on elevated basal adenosine levels in the active phase, provide sufficient adenosine to shift 3×5 mAIH-induced pLTF from a serotonin-dominant (adenosine constrained) to an adenosine-dominant (serotonin-constrained) mechanism. From another

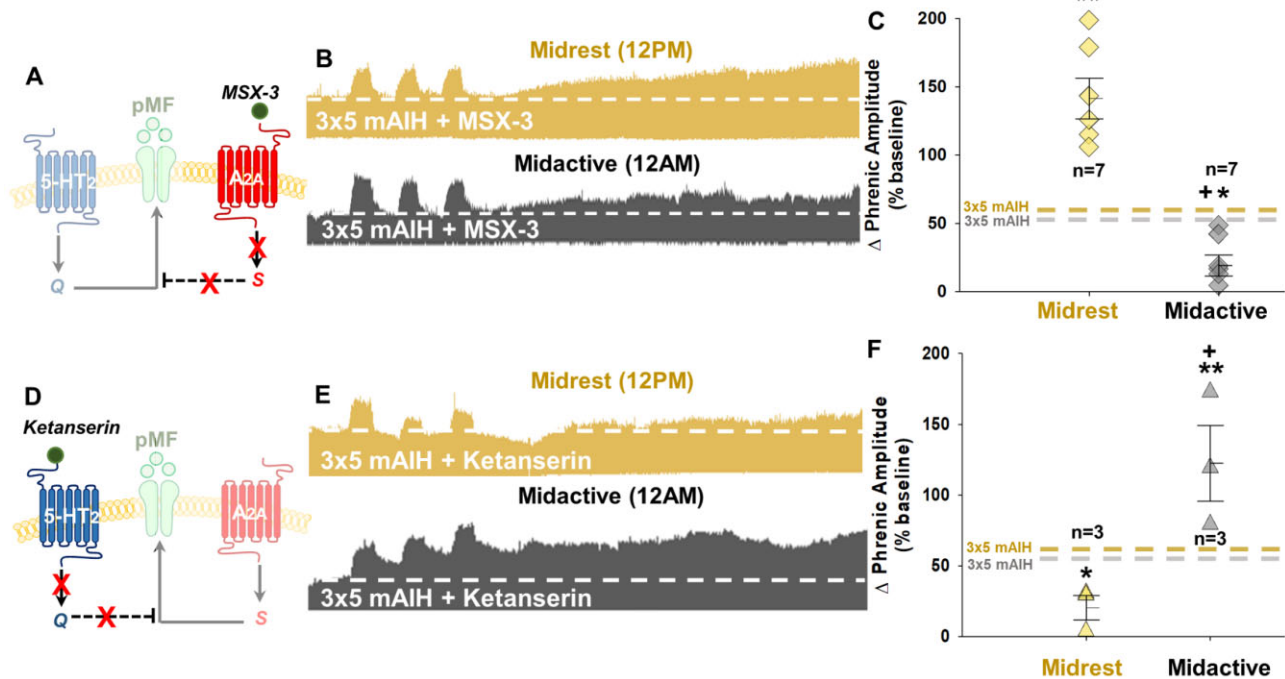


Figure 4. 3×5 mAIH induced pLTF flips from serotonin-dominant in the midrest to adenosine-dominant in the midactive phase. The adenosine A_{2A} receptor inhibitor MSX-3 was administered intrathecally at C4 15 min prior to 3×5 mAIH to minimize the adenosine constraint of serotonin-dominant plasticity during midrest (A). Representative compressed neurogram of integrated phrenic nerve activity after intrathecal MSX-3 during baseline, 3×5 mAIH (Hx1-3; PaO₂ = 40–55 mmHg), and 90 min post-mAIH (B) at midrest (12 PM; top) and midactive (12 AM; bottom) phase. During midrest, A_{2A} inhibition prior to 3×5 mAIH increases pLTF (three-way RM ANOVA, Tukey post-hoc; versus 3×5 mAIH alone, $P < .001$); in contrast, pLTF is significantly reduced by the same treatment in the midactive phase (versus 3×5 mAIH alone, $P = .007$; versus 3×5 mAIH + MSX-3 at midrest, $P < .001$; C). To verify pLTF mechanisms shift between rest and active phases, the 5-HT_{2A} receptor inhibitor, ketanserin, was given intrathecally 15 min before 3×5 mAIH (D). Compressed neurograms of integrated phrenic nerve activity after intrathecal ketanserin delivery during baseline, 3×5 mAIH protocol and 90 min post-mAIH (E) are shown in the midrest (12 PM; top) and midactive phases (12 AM; bottom). During midrest, 5-HT_{2A} receptor inhibition before 3×5 mAIH suppresses pLTF (3-way RM ANOVA, Tukey post-hoc; versus 3×5 mAIH alone, $P < .022$); the same treatment significantly enhances pLTF in the midactive phase (versus 3×5 mAIH alone, $P < .001$; versus 3×5 mAIH + ketanserin, $P < .001$; F). Bars indicate mean \pm 1 SEM; significant differences: * $P < .030$ versus 3×5 mAIH at same time of day; ** $P < .030$ versus 3×5 mAIH at same time of day and versus midactive 3×5 mAIH + MSX-3 (C) or midrest 3×5 mAIH + ketanserin (F); + $P < .001$ versus baseline.

perspective, these findings strongly suggest that one way to minimize undermining influences from hypoxia-evoked adenosine release is to shorten hypoxic episodes. Thus, we tested the hypothesis that 15, 1 min moderate hypoxic episodes elicit greater pLTF during the rest phase versus the standard 3, 5 min mAIH protocol.

Shorter Hypoxic Episodes Amplify pLTF During Midrest, but Attenuate pLTF in the Midactive Phase

To minimize adenosine accumulation during mAIH (and increase serotonin-dominant pLTF), hypoxic episode duration was shortened and presented as the 15, 1 min hypoxic episodes with 1 min intervals in the midrest and midactive phase (Figure 6A). Strikingly, the impact of 15×1 (versus 3×5) mAIH on pLTF is time-of-day dependent ($F_{1,27} = 54.814$, $P < .001$, two-way RM ANOVA; Figure 6B and C). Although phrenic amplitude 90 min post-mAIH was significantly elevated versus baseline in midrest and midactive phases in the overall ANOVA ($P < .001$ and $P = .013$, respectively; Tukey post-hoc), 15×1 mAIH-induced pLTF was greatly enhanced during midrest ($138.6 \pm 14.0\%$ pLTF; $n = 7$), reaching levels comparable to 3×5 mAIH after spinal A_{2A} receptor inhibition (Figure 4A). When this same protocol was applied during the midactive phase, mAIH elicits diminished pLTF ($30.4 \pm 4.1\%$ pLTF; $n = 7$); during the

midactive phase, 15×1 mAIH-induced pLTF was significantly less than midrest ($P < .001$; Tukey post-hoc; Cohen's $d = 3.957$), and even pLTF elicited by 3×5 mAIH during the midactive phase ($P = .021$; Cohen's $d = 2.089$). Thus, although 15×1 mAIH amplifies pLTF during midrest, when background adenosine levels are low, pLTF is constrained during the midactive phase. Although phrenic amplitude 90 min post-mAIH was significantly elevated versus baseline in both midrest and midactive phases ($P < .001$ and $P = .013$, respectively; Tukey post-hoc), 15×1 mAIH exhibits a striking time-of-day effect in contrast to similar 3×5 mAIH-induced pLTF during the midactive versus midrest phase. We hypothesize this rest/active effect arises from differential adenosine constraints on serotonin-dominant pLTF in midrest versus midactive phases.

To test this hypothesis, MSX-3 was delivered intrathecally at C4 to block cervical spinal A_{2A} receptors prior to delivering 15×1 mAIH ($n = 7$ per group; Figure 7A). There was a significant interaction between rest/active phase and MSX-3 on pLTF ($F_{5,28} = 12.05$, $P < .001$; three-way mixed effects ANOVA; Figure 7B); MSX-3 had no significant effect on 15×1 mAIH-induced pLTF during midrest ($121.5 \pm 10.7\%$ pLTF; $P = .931$; Tukey post-hoc; Cohen's $d = 0.519$), confirming enhanced midrest 15×1 mAIH-induced pLTF results from diminished hypoxia-evoked adenosine accumulation during the midrest phase, which is characterized by low background adenosine levels.

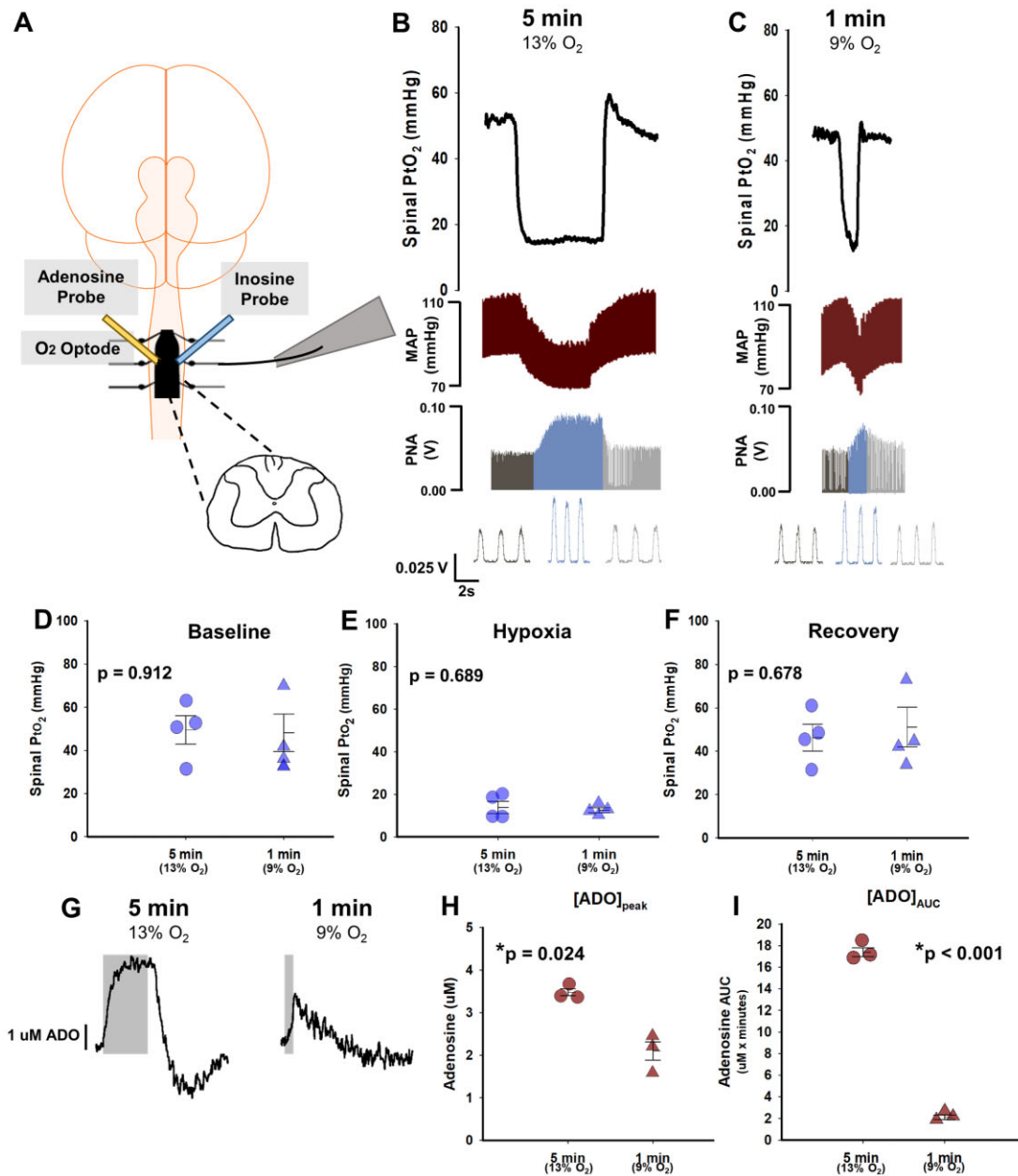


Figure 5. One minute episodes of 9% O₂ reach the same level of tissue hypoxia as 5 min, 13% O₂ episodes, yet these shorter episodes evoke less adenosine accumulation. In separate experiments, either an oxygen optode or adenosine/inosine probes were placed between ventral C3/C4 to measure changes in tissue oxygen and adenosine accumulation, respectively (A). During 5 (13% O₂; B) versus 1 min episodes (9% O₂; C), average traces illustrate similar nadirs in spinal tissue oxygen pressure (PtO₂), as well as peaks in mean arterial pressure (MAP) and phrenic nerve amplitude (PNA). There was no difference in mean spinal PtO₂ between 5 versus 1 min hypoxic episodes during baseline (D), hypoxia (E) or reoxygenation (F) ($n = 4$ per group; unpaired t-test). Despite similar reductions in arterial PO₂ and PtO₂ during 5 versus 1 min episodes, greater adenosine accumulation (μM) was observed in 5 min episodes (G; $n = 3$ per group; unpaired t-test), either when expressed as peak adenosine level ([ADO]_{peak}; H) or total area under the curve ([ADO]_{AUC}; I). Bars are means \pm 1 SEM; * $P < .030$.

During the midactive phase, A_{2A} receptor inhibition prior to 15 \times 1 mAIH markedly enhanced pLTF ($P < .001$ versus without MSX-3; Tukey post-hoc), reaching levels consistent with those observed during midrest ($163.7 \pm 26.7\%$ pLTF; $P = .591$; Cohen's $d = 2.720$; Figure 7B and C). To assure proper receptor targeting by MSX3, a second selective A_{2A} receptor inhibitor with a distinct mechanism of action, istradefylline, was used to verify effects ($n = 3$); istradefylline pretreatment during the midactive phase increased 15 \times 1 mAIH-induced pLTF versus 15 \times 1 mAIH alone ($P < .001$; Tukey post-hoc; Cohen's $d = 0.519$), consistent

with MSX-3 ($193.1 \pm 56.6\%$ pLTF; $P = .882$, Tukey post-hoc; Cohen's $d = 2.335$; Figure 7D and G).

Finally, intrathecal ketanserin was administered to block cervical spinal 5-HT_{2A/C} receptors prior to 15 \times 1 mAIH during midrest ($n = 3$; Figure 7E) to confirm that pLTF was serotonin-driven. As expected, ketanserin blocked pLTF ($-7.9\% \pm 10.8\%$ pLTF; $P = .692$ versus baseline; Tukey post-hoc; Figure 7F), and was significantly lower than 15 \times 1 mAIH alone ($P < .001$; Tukey post-hoc; Cohen's $d = 4.987$; Figure 7G). Thus, mAIH consisting of shorter hypoxic episodes drives serotonin-dominant plasticity

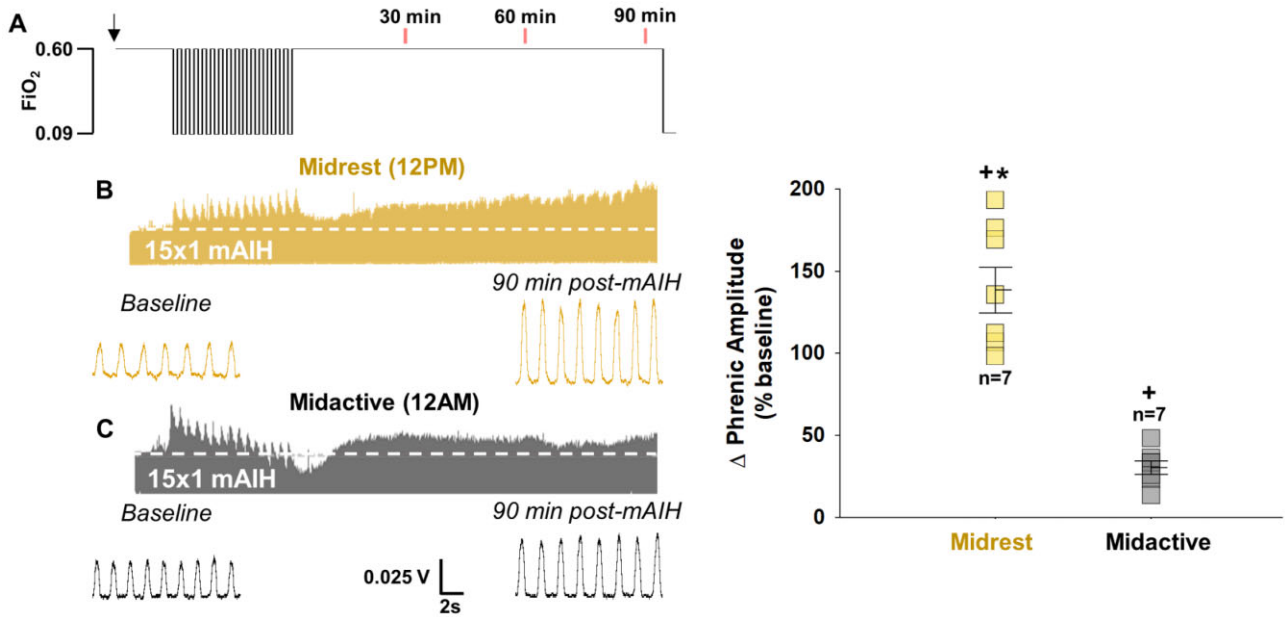


Figure 6. With 15 × 1 mAIH, pLTF is enhanced during midrest (noon) but suppressed during midactive phase (midnight). With the 15 × 1 mAIH protocol (A), compressed integrated phrenic responses are shown during baseline, 15 × 1 mAIH, and 90 min post-mAIH at midrest (12 PM; B) and midactive (12 AM; C) phase. Phrenic burst amplitude, represented as % change from baseline at 90 min post 15 × 1 mAIH, is substantially different during midrest versus midactive phases (n = 7 per group; three-way RM ANOVA, P < .001). Bars show means ± 1 SEM. Significant differences for: *P < .001, versus midactive 15 × 1 mAIH; +P < .020, versus baseline. FiO₂, fraction of inspired oxygen; mAIH, moderate acute intermittent hypoxia.

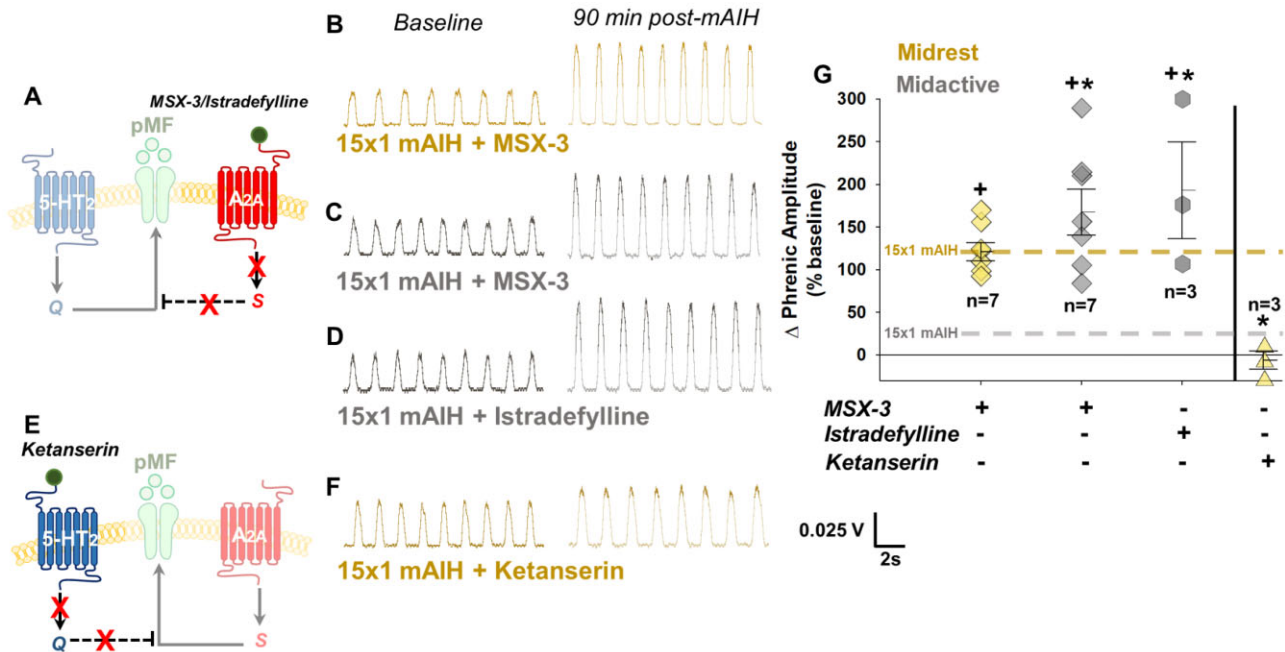


Figure 7. Following 15 × 1 mAIH, pLTF is serotonin-driven during both midrest and midactive phases. Adenosine 2A receptor (A_{2A}) inhibition with MSX-3 (intrathecal at C4 15 min prior to 15 × 1 mAIH) was used to minimize any adenosinergic constraint on serotonin-driven plasticity (A). Compressed integrated phrenic neurograms after intrathecal MSX-3 are shown during baseline and 90 min post-mAIH for midrest (12 PM; B) and midactive phase (12 AM; C). Compressed integrated phrenic neurograms are shown after intrathecal delivered istradefylline, another selective A_{2A} receptor inhibitor, during baseline and 90 min post-mAIH during the midactive phase (D). Representative neurograms of integrated phrenic nerve activity after intrathecal ketanserin (E) during baseline and 90 min post-15 × 1 mAIH at midrest confirm serotonin-dependent pLTF during midrest and midactive phases (F). During midrest, A_{2A} receptor inhibition prior to 15 × 1 mAIH (n = 7) had no effect on pLTF (three-way mixed effects ANOVA, Tukey post-hoc; versus 15 × 1 mAIH alone, P = .931; G), although pLTF was restored in the midactive phase (n = 7) to levels observed during midrest (versus 15 × 1 mAIH alone, P < .001; versus 15 × 1 mAIH + MSX-3 at midrest, P = .123); A_{2A} receptor specificity was confirmed with istradefylline (n = 3; midactive 15 × 1 mAIH + MSX-3 versus istradefylline, P = .882). Further, pLTF during midrest 15 × 1 mAIH was significantly reduced by ketanserin versus midrest 15 × 1 mAIH alone (n = 3; P < .001). Bars show means ± 1 SEM; Significant differences: *P < .001 versus respective midrest or midactive 15 × 1 mAIH; +P < .001 versus baseline.

during both midrest and midactive phases, although elevated basal adenosine levels during the active phase undermine serotonin-dominant plasticity.

Discussion

We demonstrate that adenosine is a powerful regulator of mAIH-induced phrenic motor plasticity across the daily rest/active cycle, and that its specific impact depends on the AIH protocol used. Shifts in basal levels and hypoxia-evoked adenosine release combine to regulate the serotonin/adenosine balance and, thus, the magnitude and mechanism driving plasticity. Since AIH-induced pLTF is an important model of respiratory motor plasticity in a critical neural system necessary for life (breathing), knowledge of factors regulating pLTF has considerable importance with respect to future experimental design, and our understanding of mechanisms and the biological significance of AIH-induced phrenic motor plasticity. Beyond that, increased understanding of pLTF advances our knowledge of neuroplasticity in general.

From a very different perspective, studies of AIH-induced pLTF have inspired translational efforts in two respects: (1) as a model for AIH-induced plasticity in other respiratory and non-respiratory motor systems^{4,6}; and (2) as inspiration for clinical trials attempting to harness AIH as a therapeutic modality to elicit plasticity and functional recovery of respiratory and non-respiratory motor impairment in people with chronic spinal cord injury^{4,5} and ALS.⁷ Indeed, therapeutic AIH is emerging as a simple, safe, and effective treatment to restore breathing⁴⁸ and non-respiratory movements such as walking⁴⁹ and hand/arm function^{50,51} in people living with chronic spinal cord injury. We now demonstrate that it is essential to consider AIH protocol details and delivery in the rest versus active cycle in clinical trial design since humans (diurnal) and rats (nocturnal) have reverse rest/active phases. This is particularly important since rodent studies inspiring translation are most often performed in the midrest phase, whereas human trials are typically performed in the midactive phase. Although the importance of rest/active phase has yet to be considered in those trials, our findings may represent a “game changer” since daily rest/active cycle can shift both the magnitude and mechanism of pLTF in an AIH protocol-specific manner. Although it is easy to understand the significance of outcome magnitude, the impact of shifts in driving mechanism are not yet clear. However, details of the intracellular signaling cascades driving serotonin versus adenosine-dependent phrenic motor plasticity suggest the potential for differential impact on other important outcomes, such as synaptogenesis, axon growth, or other properties of the neural circuit.

Impact of Adenosine on pLTF

During the past two decades, major advances have been made in our mechanistic understanding of mAIH-induced plasticity in the phrenic motor system, a motor system once thought of as fixed and immutable. Despite such progress, virtually no attention has been given to potential rest/active (or circadian) effects on plasticity. Since rodents are nocturnal, studies in rodent models pose a dilemma as a model for diurnal humans. Most rodent and human studies of AIH-induced plasticity occur during the day, in an opposite activity state than humans. Correcting this oversight has major implications for our understanding and application of AIH-induced respiratory motor plasticity.

During the rest phase, basal spinal adenosine levels are low (Figure 2), and peak adenosine levels are a function of both

the severity and duration of hypoxic episodes (ie, 3×5 versus 15×1 min episodes). Since shorter hypoxic episodes reduce evoked adenosine release (Figure 5), adenosine constraints on serotonin-dominant plasticity are minimized with the 15×1 versus 3×5 mAIH protocol. Thus, spinal A_{2A} receptor inhibition during the rest phase has negligible impact on 15×1 mAIH-induced pLTF (Figure 7), but nearly doubles pLTF after 3×5 mAIH, reaching levels comparable to the 15×1 protocol (Figure 4) by releasing the adenosine “brake” imposed by longer-hypoxic episodes (Figures 5 and 8). In striking contrast, elevated background adenosine levels during the active phase suppress 15×1 mAIH-induced pLTF (Figure 6).

Since the “standard” 3×5 mAIH protocol triggers greater hypoxia-evoked adenosine release (versus 15×1), we suggest the 3×5 mAIH protocol delivered during the midactive phase combines with elevated background adenosine levels, establishing adenosine levels sufficient to flip from serotonin-dominant (midrest) to adenosine-dominant plasticity (midactive; Figure 3). Thus, adenosine constrains or dominates phrenic motor plasticity depending on: (1) the duration of hypoxic episodes in the mAIH protocol; and (2) delivery of AIH in the rest versus active phase. To our knowledge, a similar “mechanistic flip” that depends on rest/active phase and inducing protocol has never been demonstrated in any other form of neuroplasticity.

Adenosine links brain activity state with the sleep-wake cycle and neuroplasticity.⁵² Regarding spinal respiratory neuroplasticity, the impact of adenosine across the daily rest/active cycle was previously unknown. We now demonstrate a fundamental link between daily spinal adenosine fluctuations and phrenic motor plasticity, an impact modified by hypoxia evoked-adenosine release/accumulation. Adenosine influences pLTF via A_{2A} receptor activation, initiating intracellular signaling cascades that inhibit the serotonin-dependent, Q pathway or, at the extreme, drive a distinct mechanism of plasticity.^{16,53–55}

Hypoxia-evoked adenosine release from spinal glia has been proposed to depend on the severity and duration of hypoxic episodes based on indirect evidence^{16,20}; in the present study, we directly demonstrate increased adenosine accumulation during longer (5 min) versus shorter (1 min) hypoxic episodes, despite similar levels of arterial and tissue hypoxia (Figure 5). Evoked adenosine release occurs on shifting baseline adenosine levels across the rest/active cycle. Although it is well known that brain extracellular adenosine levels increase during prolonged wakefulness, and decrease during sleep/rest,^{29,33,56} we demonstrate similar time-dependent shifts in ventral cervical spinal cord encompassing the phrenic motor nucleus (Figure 2). These findings suggest that baseline and evoked adenosine levels must both be considered when evaluating adenosine regulation of AIH-induced phrenic motor plasticity (Figure 8).

Additional triggers to adenosine accumulation in the ventral cervical spinal cord may contribute to the overall “adenosine burden,” including neuroinflammation,⁵⁷ aging,^{58–60} or spinal cord injury.³⁹ Each of these factors is known to undermine mAIH induced pLTF,^{61,62} although the potential role of adenosine and their actions has only recently been discovered.^{63,64}

The Potential to Harness Serotonin- Versus Adenosine-Dependent Plasticity

Although serotonin and adenosine are capable of eliciting phenotypically similar pLTF, it is not yet known if these cellular cascades differentially impact other outcomes, such as axonal growth, synaptogenesis or neuroprotection. Indeed,

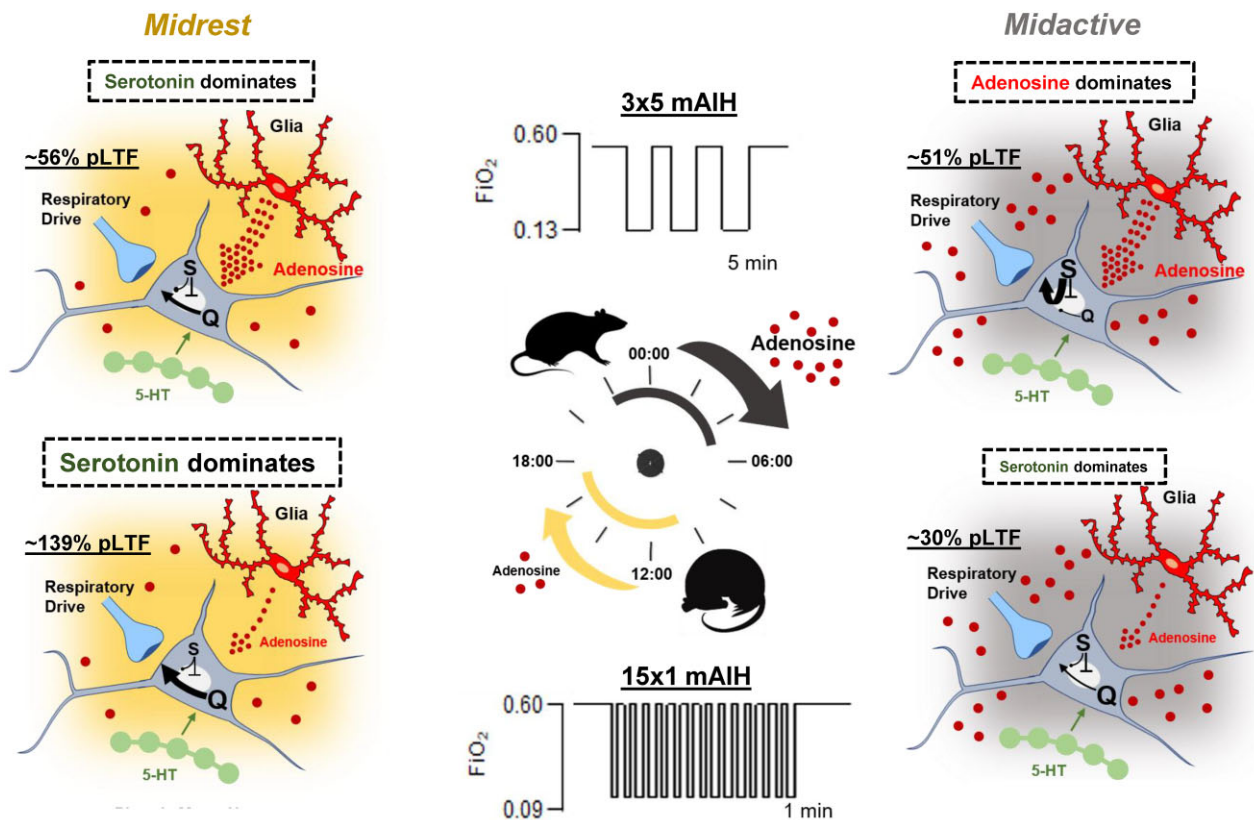


Figure 8. mAIH-induced pLTF is regulated by time-of-day dependent shifts in basal adenosine levels and hypoxic episode duration (ie, evoked adenosine release). Spinal adenosine (red dots) fluctuates across the daily rest/active cycle, with low levels during the rest phase (yellow) and elevated levels in the active phase (gray background). In the top row, 3, 5 min episodes of moderate hypoxia (3×5 mAIH) evoke greater adenosine release from glia (signified by larger dotted arrows). In the rest phase (top row, left panel), 3×5 mAIH induces pLTF through a serotonin-dominant (Q pathway), adenosine constrained mechanism. In the active phase (top row, right panel), greater basal adenosine levels near phrenic motor neurons coupled with still high hypoxia-evoked adenosine release cause a mechanistic flip; 3×5 mAIH now induces pLTF through an adenosine-dominant (S pathway), serotonin constrained mechanism. In the bottom row, 15, 1 min episodes of moderate hypoxia (15×1 mAIH) evoke minimal adenosine release (signified by smaller arrow from glia). In the rest phase (bottom row, left panel), 15×1 mAIH elicits pLTF through the full-blown serotonin-dependent Q pathway, with minimal adenosine constraint. However, in the active phase (bottom row, right panel), 15×1 mAIH still elicits pLTF through the Q pathway, but is now undermined considerably by elevated basal adenosine levels; in this case, 15×1 mAIH does not reach the threshold adenosine level necessary to flip pLTF from the Q to the S pathway, yet the Q pathway is sufficiently undermined to be lower than S-pathway driven 3×5 mAIH-induced pLTF at this time.

each plasticity mechanism is driven by molecules associated with distinct neural behaviors such as synaptogenesis⁶⁵ versus axonal growth,⁶⁶ respectively. For example, the S pathway requires Akt and mTORC1 signaling,^{26,54,67} a pathway commonly associated with axonal growth/elongation.⁶⁶ Conversely, the Q pathway requires ERK MAPK and BDNF/TrkB signaling,^{37,68–70} a pathway commonly associated with axon sprouting and synaptogenesis.⁶⁵ The ability to elicit different mechanisms of plasticity based on rest/activity phase and AIH protocol creates the potential to target these distinct outcomes for more impactful therapeutics.

Limitations

This body of work represents a unique combination of approaches that include in vivo neurophysiology, oxygen optodes, adenosine microbiosensors and assays, targeted pharmacologic manipulations of cervical spinal receptors, and complex time-of-day-based physiology. Collectively, these approaches justified a new conceptual framework concerning the dynamical interplay between chemoreceptor activated neural networks (serotonin) versus local tissue oxygen effects (ATP/adenosine release) in AIH-induced phrenic motor plasticity. Since this framework includes previously unrecognized (and

powerful) time-of-day and mAIH protocol effects, our results constitute a major advance in understanding spinal motor plasticity.

On the other hand, neuromodulators other than adenosine fluctuate during the sleep/wake cycle and could provide distinct influences on pLTF, including corticosterone,⁷¹ melatonin^{72,73} and orexin,⁷⁴ among others. Nevertheless, adenosine is likely the primary effector since A_{2A} receptor inhibition had direct effects on pLTF during both midrest and midactive experiments. Going forward, it is essential to consider protocol specific time-of-day or rest/activity phase effects in the design of experiments and clinical trial design as we attempt to harness AIH as a therapeutic modality to restore breathing and other movements in people living with chronic spinal cord injury, ALS, and other neuromuscular disorders that compromise breathing and other motor behaviors.

Though we present clear evidence for the role of basal spinal adenosine in mediating time-of-day shifts in pLTF magnitude and mechanism, hypoxia-evoked adenosine release in ventral C4 spinal cord was measured late in the rest or early active phase. In rodent basal forebrain (*in vitro*), AMPA-evoked adenosine release is greater in the active phase versus the rest phase⁴²; although this report supports our findings, it is important to verify if similar time-of-day effects occur in hypoxia-evoked spinal adenosine release.

Since all rats used in this study were male, we cannot comment on the generalizability of our findings to females. However, female rats exhibit a profound age- and estrus cycle dependent sexual dimorphism in mAIH-induced pLTF.^{62,75,76} Although it is not known how sex steroid hormones influence pLTF across the rest/active cycle, sleep duration and adenosine levels across the daily rest/active cycle are differentially affected through the estrus cycle.⁷⁷ Sex and age effects were beyond the scope of this study and warrant future investigation.

In vivo neurophysiology preparations require anesthesia, which can disrupt circadian rhythms.^{78,79} From induction to urethane conversion, rats in this study were exposed to progressively decreasing isoflurane concentrations over ~1 h. Isoflurane shifts circadian phase when delivered during the active phase in rats, but has minimal impact during the rest phase.⁸⁰ Such isoflurane-induced phase shifts occur days after initial exposure and shift the “clock” by < 1.5 h.^{80,81} Since the total time of our experiments is ~4–5 h, and hippocampal neurotransmitter release returns to normal by 4 h after discontinuing isoflurane,⁸⁰ there is little evidence that isoflurane, used as an inducing agent, had any major impact on the results of this study.

Urethane anesthesia is most often used in our neuroplasticity studies since it creates a stable, long-lasting anesthetic state yet maintains brain functional connectivity versus unanesthetized rats.⁸² Urethane is unique among anesthetics since, at lower doses, it permits spontaneous shifts between REM-like and nonREM-like EEG states, with corresponding changes in physiological variables typically associated with natural sleep.^{83–86} Indeed, the ability for urethane to mimic natural sleep is consistent with reports that: (1) anesthesia exerts lesser time-of-day-effects when delivered in the rest versus active phase,^{78,80,81} which would minimize differences between rest versus active phase in the present study; and (2) urethane anesthetized rats exhibit similar EEG-state dependence of ventilatory LTF⁶⁶ versus natural sleep,^{87,88} suggesting that EEG state changes under urethane anesthesia and natural sleep impart similar physiological effects on phrenic motor plasticity. Further, since light cues are the most powerful influencer of circadian rhythm and the rest/active cycle,^{89–92} and urethane anesthesia preserves photoreponsiveness,⁹³ our results are unlikely anesthesia-related.

Translational Significance

Phrenic LTF is a model of respiratory motor plasticity that has guided translation to people living with chronic spinal cord injury and ALS (see below), as well as to nonrespiratory motor systems (walking, arm/hand function). We are currently engaged in a “translational flywheel,” where rodent experiments drive human studies of therapeutic AIH, which then inform the need for further rodent studies.⁴ Indeed, several clinical trials are currently underway, exploring the ability of mAIH to restore breathing, walking, and hand/arm function in people living with chronic spinal cord injury and ALS. However, these trials suffer from lack of full mechanistic understanding as we strive to optimize mAIH as a therapeutic modality. Based on the present findings, AIH protocol and time-of-day (rest/active phase) are highly relevant variables. Therefore, we must reconsider the current practice of applying therapeutic AIH during the human active phase since these findings suggest the 15 × 1 mAIH protocol during the rest phase would produce maximum pLTF/respiratory motor output, but minimum pLTF in the active phase. Alternately, we need to mitigate influence of elevated adenosine via

pretreatment with A_{2A} receptor inhibitors. Regardless, consideration of adenosine and time-of-day in future clinical trials is of major importance.

Conclusion

In summary, using the “conventional” 3 × 5 mAIH protocol, we demonstrate a complete shift in the mechanism driving mAIH-induced pLTF from serotonin-dominance in the midrest phase to adenosine-dominance in the midactive phase. This shift is driven by fluctuations in spinal adenosine levels across the rest/active cycle, combined with hypoxia-evoked adenosine release. However, with a refined protocol consisting of 15, 1 min hypoxic episodes, pLTF is greatly enhanced during the rest phase (versus 3 × 5 AIH), but attenuated during the active phase due to greater adenosine constraint to serotonin-dominant pLTF. The present studies are the first to demonstrate: (1) basal adenosine changes between the rest versus active phase in spinal tissues containing the phrenic motor nucleus; (2) the powerful role of adenosine in regulating pLTF across the daily rest/active cycle; and (3) the importance of mAIH episode duration and its dependence on the rest/active cycle. These findings greatly advance our understanding of mechanisms regulating AIH-induced motor plasticity, and provide new guidance for future experimental and clinical trial design.

Acknowledgments

The authors would like to thank J. Oberto and C. Lurk for their technical assistance.

Author Contributions

A.B.M., M.N.K., and G.S.M.: conceptualization; A.B.M., Y.B.S., R.R.P., and G.S.M.: data curation; A.B.M. and G.S.M.: formal analysis; G.S.M.: funding acquisition; A.B.M., Y.B.S., M.N.K., R.R.P., and G.S.M.: investigation; A.B.M. and G.S.M.: methodology; G.S.M.: supervision; A.B.M. and G.S.M.: writing (original draft); and A.B.M., Y.B.S., M.N.K., R.R.P., and G.S.M.: manuscript revisions.

Supplementary Material

Supplementary material is available at the *APS Function* online.

Funding

This work was supported by the NIH R01HL148030 (G.S.M.), NIH R01HL149800 (G.S.M.), and NIH T32HL134621-5 (A.B.M., M.N.K.), and the UF Brain Spinal Cord Research Trust Fund.

Conflict of Interest

None declared.

Data Availability

All data needed to evaluate the conclusions presented are available in the paper and/or the Supplementary Materials.

References

- Mitchell GS, Johnson SM. Neuroplasticity in respiratory motor control. *J Appl Physiol* (1985). 2003;94(1):358–374.

2. Mitchell GS, Baker TL. Respiratory neuroplasticity: mechanisms and translational implications of phrenic motor plasticity. *Handb Clin Neurol*. 2022;**188**:409–432.
3. Mitchell GS, Baker TL, Nanda SA, et al. Invited review: intermittent hypoxia and respiratory plasticity. *J Appl Physiol* (1985). 2001;**90**(6):2466–2475.
4. Vose AK, Welch JF, Nair J, et al. Therapeutic acute intermittent hypoxia: a translational roadmap for spinal cord injury and neuromuscular disease. *Exp Neurol*. 2022;**347**:113891.
5. Gonzalez-Rothi EJ, Lee KZ, Dale EA, Reier PJ, Mitchell GS, Fuller DD. Intermittent hypoxia and neurorehabilitation. *J Appl Physiol* (1985). 2015;**119**(12):1455–1465.
6. Dale EA, Ben Mabrouk F, Mitchell GS. Unexpected benefits of intermittent hypoxia: enhanced respiratory and nonrespiratory motor function. *Physiology (Bethesda)*. 2014;**29**(1):39–48.
7. Sajjadi E, Seven YB, Ehrbar JG, Wymer JP, Mitchell GS, Smith BK. Acute intermittent hypoxia and respiratory muscle recruitment in people with amyotrophic lateral sclerosis: a preliminary study. *Exp Neurol*. 2022;**347**:113890.
8. Millhorn DE, Eldridge FL, Waldrop TG. Prolonged stimulation of respiration by a new central neural mechanism. *Respir Physiol*. 1980;**41**(1):87–103.
9. Hayashi F, Coles SK, Bach KB, Mitchell GS, McCrimmon DR. Time-dependent phrenic nerve responses to carotid afferent activation: intact vs. decerebellate rats. *Am J Physiol*. 1993;**265**(4 Pt 2):R811–819.
10. Fregosi RF, Mitchell GS. Long-term facilitation of inspiratory intercostal nerve activity following carotid sinus nerve stimulation in cats. *J Physiol*. 1994;**477**(Pt 3):469–479.
11. Feldman JL, Mitchell GS, Nattie EE. Breathing: rhythmicity, plasticity, chemosensitivity. *Annu Rev Neurosci*. 2003;**26**(1):239–266.
12. Millhorn DE, Eldridge FL, Waldrop TG. Prolonged stimulation of respiration by endogenous central serotonin. *Respir Physiol*. 1980;**42**(3):171–188.
13. Bach KB, Mitchell GS. Hypoxia-induced long-term facilitation of respiratory activity is serotonin dependent. *Respir Physiol*. 1996;**104**(2–3):251–260.
14. Baker-Herman TL, Mitchell GS. Phrenic long-term facilitation requires spinal serotonin receptor activation and protein synthesis. *J Neurosci*. 2002;**22**(14):6239–6246.
15. Tadjalli A, Mitchell GS. Cervical spinal 5-HT_{2A} and 5-HT_{2B} receptors are both necessary for moderate acute intermittent hypoxia-induced phrenic long-term facilitation. *J Appl Physiol* (1985). 2019;**127**(2):432–443.
16. Nichols NL, Dale EA, Mitchell GS. Severe acute intermittent hypoxia elicits phrenic long-term facilitation by a novel adenosine-dependent mechanism. *J Appl Physiol* (1985). 2012;**112**(10):1678–1688.
17. Seven YB, Perim RR, Hobson OR, Simon AK, Tadjalli A, Mitchell GS. Phrenic motor neuron adenosine 2A receptors elicit phrenic motor facilitation. *J Physiol*. 2018;**596**(8):1501–1512.
18. Fields DP, Mitchell GS. Divergent cAMP signaling differentially regulates serotonin-induced spinal motor plasticity. *Neuropharmacology*. 2017;**113**(Pt A):82–88.
19. Perim RR, Mitchell GS. Circulatory control of phrenic motor plasticity. *Respir Physiol Neurobiol*. 2019;**265**:19–23.
20. Devinney MJ, Nichols NL, Mitchell GS. Sustained hypoxia elicits competing spinal mechanisms of phrenic motor facilitation. *J Neurosci*. 2016;**36**(30):7877–7885.
21. Winn HR, Rubio R, Berne RM. Brain adenosine concentration during hypoxia in rats. *Am J Physiol*. 1981;**241**(2):H235–242.
22. Martin ED, Fernandez M, Perea G, et al. Adenosine released by astrocytes contributes to hypoxia-induced modulation of synaptic transmission. *Glia*. 2007;**55**(1):36–45.
23. Hoffman MS, Golder FJ, Mahamed S, Mitchell GS. Spinal adenosine A₂(A) receptor inhibition enhances phrenic long term facilitation following acute intermittent hypoxia. *J Physiol* 2010;**588**(Pt 1):255–266.
24. Perim RR, Fields DP, Mitchell GS. Cross-talk inhibition between 5-HT_{2B} and 5-HT₇ receptors in phrenic motor facilitation via NADPH oxidase and PKA. *Am J Physiol Regul Integr Comp Physiol*. 2018;**314**(5):R709–R715.
25. Perim RR, Fields DP, Mitchell GS. Protein kinase cdelta constrains the S-pathway to phrenic motor facilitation elicited by spinal 5-HT₇ receptors or severe acute intermittent hypoxia. *J Physiol*. 2019;**597**(2):481–498.
26. Nichols NL, Mitchell GS. Mechanisms of severe acute intermittent hypoxia-induced phrenic long-term facilitation. *J Neurophysiol*. 2021;**125**(4):1146–1156.
27. Porkka-Heiskanen T, Strecker RE, McCarley RW. Brain site-specificity of extracellular adenosine concentration changes during sleep deprivation and spontaneous sleep: an in vivo microdialysis study. *Neuroscience*. 2000;**99**(3):507–517.
28. Bjorness TE, Greene RW. Adenosine and sleep. *Curr Neuropharmacol*. 2009;**7**(3):238–245.
29. Huang ZL, Urade Y, Hayaishi O. The role of adenosine in the regulation of sleep. *Curr Top Med Chem*. 2011;**11**(8):1047–1057.
30. Porkka-Heiskanen T, Strecker RE, Thakkar M, Bjorkum AA, Greene RW, McCarley RW. Adenosine: a mediator of the sleep-inducing effects of prolonged wakefulness. *Science*. 1997;**276**(5316):1265–1268.
31. Tester NJ, Fuller DD, Fromm JS, Spiess MR, Behrman AL, Mateika JH. Long-term facilitation of ventilation in humans with chronic spinal cord injury. *Am J Respir Crit Care Med*. 2014;**189**(1):57–65.
32. Tester NJ, Fuller DD, Mateika JH. Ventilatory long-term facilitation in humans. *Am J Respir Crit Care Med*. 2014;**189**(8):1009–1010.
33. Jagannath A, Varga N, Dallmann R, et al. Adenosine integrates light and sleep signalling for the regulation of circadian timing in mice. *Nat Commun*. 2021;**12**(1):2113.
34. Jimenez-Zarate BS, Pina-Leyva C, Rodriguez-Sanchez M, Floran-Garduno B, Jimenez-Zamudio LA, Jimenez-Estrada I. Day-night variations in the concentration of neurotransmitters in the rat lumbar spinal cord. *J Circadian Rhythms*. 2021;**19**(1):9.
35. Perim RR, Kubilis PS, Seven YB, Mitchell GS. Hypoxia-induced hypotension elicits adenosine-dependent phrenic long-term facilitation after carotid denervation. *Exp Neurol*. 2020;**333**:113429.
36. Agosto-Marlin IM, Nichols NL, Mitchell GS. Adenosine-dependent phrenic motor facilitation is inflammation resistant. *J Neurophysiol*. 2017;**117**(2):836–845.
37. Tadjalli A, Seven YB, Perim RR, Mitchell GS. Systemic inflammation suppresses spinal respiratory motor plasticity via mechanisms that require serine/threonine protein phosphatase activity. *J Neuroinflammation*. 2021;**18**(1):28.
38. Zabka AG, Behan M, Mitchell GS. Long term facilitation of respiratory motor output decreases with age in male rats. *J Physiol*. 2001;**531**(Pt 2):509–514.
39. Perim RR, Gonzalez-Rothi EJ, Mitchell GS. Cervical spinal injury compromises caudal spinal tissue oxygenation and undermines acute intermittent hypoxia-induced phrenic long-term facilitation. *Exp Neurol*. 2021;**342**:113726.

40. McGuire M, Zhang Y, White DP, Ling L. Phrenic long-term facilitation requires NMDA receptors in the phrenic motoneuron in rats. *J Physiol*. 2005;567(Pt 2):599–611.
41. Kelly MN, Smith DN, Sunshine MD, et al. Circadian clock genes and respiratory neuroplasticity genes oscillate in the phrenic motor system. *Am J Physiol Regul Integr Comp Physiol*. 2020;318(6):R1058–R1067.
42. Sims RE, Wu HH, Dale N. Sleep-wake sensitive mechanisms of adenosine release in the basal forebrain of rodents: an in vitro study. *PLoS One*. 2013;8(1):e53814.
43. Zhang Z, Wang HJ, Wang DR, Qu WM, Huang ZL. Red light at intensities above 10 lx alters sleep-wake behavior in mice. *Light Sci Appl*. 2017;6(5):e16231.
44. Perim RR, El-Chami M, Gonzalez-Rothi EJ, Mitchell GS. Baseline arterial CO₂ pressure regulates acute intermittent hypoxia-induced phrenic long-term facilitation in rats. *Front Physiol*. 2021;12:573385.
45. Harada Y, Kuno M, Wang YZ. Differential effects of carbon dioxide and pH on central chemoreceptors in the rat in vitro. *J Physiol*. 1985;368(1):679–693.
46. Mateika JH, Fregosi RF. Long-term facilitation of upper airway muscle activities in vagotomized and vagally intact cats. *J Appl Physiol* (1985). 1997;82(2):419–425.
47. Kumar P, Prabhakar NR. Peripheral chemoreceptors: function and plasticity of the carotid body. *Compr Physiol*. 2012;2(1):141–219.
48. Sutor T, Cavka K, Vose AK, et al. Single-session effects of acute intermittent hypoxia on breathing function after human spinal cord injury. *Exp Neurol* 2021;342:113735.
49. Hayes HB, Jayaraman A, Herrmann M, Mitchell GS, Rymer WZ, Trumbower RD. Daily intermittent hypoxia enhances walking after chronic spinal cord injury: a randomized trial. *Neurology*. 2014;82(2):104–113.
50. Trumbower RD, Hayes HB, Mitchell GS, Wolf SL, Stahl VA. Effects of acute intermittent hypoxia on hand use after spinal cord trauma: a preliminary study. *Neurology*. 2017;89(18):1904–1907.
51. Sandhu MS, Perez MA, Oudega M, Mitchell GS, Rymer WZ. Efficacy and time course of acute intermittent hypoxia effects in the upper extremities of people with cervical spinal cord injury. *Exp Neurol*. 2021;342:113722.
52. Bannon NM, Chistiakova M, Chen JY, Bazhenov M, Volgushev M. Adenosine shifts plasticity regimes between associative and homeostatic by modulating heterosynaptic changes. *J Neurosci*. 2017;37(6):1439–1452.
53. Dale-Nagle EAHM, MacFarlane PM, Mitchell GS. Multiple pathways to long-lasting phrenic motor facilitation. *Adv Exp Med Biol*. 2010;669:225–230.
54. Golder FJ, Ranganathan L, Satriotomo I, et al. Spinal adenosine A_{2a} receptor activation elicits long-lasting phrenic motor facilitation. *J Neurosci*. 2008;28(9):2033–2042.
55. Navarrete-Opazo A, Dougherty BJ, Mitchell GS. Enhanced recovery of breathing capacity from combined adenosine 2A receptor inhibition and daily acute intermittent hypoxia after chronic cervical spinal injury. *Exp Neurol*. 2017;287(Pt 2):93–101.
56. Kell CA, Stehle JH. Just the two of us: melatonin and adenosine in rodent pituitary function. *Ann Med*. 2005;37(2):105–120.
57. Imura Y, Morizawa Y, Komatsu R, et al. Microglia release ATP by exocytosis. *Glia*. 2013;61(8):1320–1330.
58. Sebastiao AM, Cunha RA, de Mendonca A, Ribeiro JA. Modification of adenosine modulation of synaptic transmission in the hippocampus of aged rats. *Br J Pharmacol*. 2000;131(8):1629–1634.
59. Costenla AR, Diogenes MJ, Canas PM, et al. Enhanced role of adenosine A_{2A} receptors in the modulation of LTP in the rat hippocampus upon ageing. *Eur J Neurosci*. 2011;34(1):12–21.
60. Canas PM, Duarte JM, Rodrigues RJ, Kofalvi A, Cunha RA. Modification upon aging of the density of presynaptic modulation systems in the hippocampus. *Neurobiol Aging*. 2009;30(11):1877–1884.
61. Huxtable AG, Smith SM, Vinit S, Watters JJ, Mitchell GS. Systemic LPS induces spinal inflammatory gene expression and impairs phrenic long-term facilitation following acute intermittent hypoxia. *J Appl Physiol* (1985). 2013;114(7):879–887.
62. Behan M, Zabka AG, Mitchell GS. Age and gender effects on serotonin-dependent plasticity in respiratory motor control. *Respir Physiol Neurobiol*. 2002;131(1–2):65–77.
63. Marciante AB, Mitchell GS. Mild inflammation impairs acute intermittent hypoxia-induced phrenic long-term facilitation by a spinal adenosine-dependent mechanism. *J Neurophysiol* 2023;129(3):799–806.
64. Marciante AB, Mitchell GS. Increased spinal adenosine impairs phrenic long-term facilitation in aging rats. *J Appl Physiol* (1985). 2023;134(6):1537–1548.
65. Martinez A, Alcantara S, Borrell V, et al. TrkB and TrkC signaling are required for maturation and synaptogenesis of hippocampal connections. *J Neurosci*. 1998;18(18):7336–7350.
66. Miao L, Yang L, Huang H, Liang F, Ling C, Hu Y. mTORC1 is necessary but mTORC2 and GSK3beta are inhibitory for AKT3-induced axon regeneration in the central nervous system. *Elife* 2016;5:e14908.
67. Perim RR, Fields DP, Mitchell GS. Spinal AMP kinase activity differentially regulates phrenic motor plasticity. *J Appl Physiol* (1985). 2020;128(3):523–533.
68. Baker-Herman TL, Fuller DD, Bavis RW, et al. BDNF is necessary and sufficient for spinal respiratory plasticity following intermittent hypoxia. *Nat Neurosci*. 2004;7(1):48–55.
69. Hoffman MS, Nichols NL, Macfarlane PM, Mitchell GS. Phrenic long-term facilitation after acute intermittent hypoxia requires spinal ERK activation but not TrkB synthesis. *J Appl Physiol* (1985). 2012;113(8):1184–1193.
70. Dale EA, Fields DP, Devinney MJ, Mitchell GS. Phrenic motor neuron TrkB expression is necessary for acute intermittent hypoxia-induced phrenic long-term facilitation. *Exp Neurol*. 2017;287(Pt 2):130–136.
71. Mohawk JA, Pargament JM, Lee TM. Circadian dependence of corticosterone release to light exposure in the rat. *Physiol Behav*. 2007;92(5):800–806.
72. Chaudhury D, Wang LM, Colwell CS. Circadian regulation of hippocampal long-term potentiation. *J Biol Rhythms*. 2005;20(3):225–236.
73. Dauchy RT, Wren MA, Dauchy EM, et al. The influence of red light exposure at night on circadian metabolism and physiology in Sprague-Dawley rats. *J Am Assoc Lab Anim Sci*. 2015;54(1):40–50.
74. Terada J, Nakamura A, Zhang W, et al. Ventilatory long-term facilitation in mice can be observed during both sleep and wake periods and depends on orexin. *J Appl Physiol* (1985). 2008;104(2):499–507.
75. Zabka AG, Behan M, Mitchell GS. Selected contribution: time-dependent hypoxic respiratory responses in female

- rats are influenced by age and by the estrus cycle. *J Appl Physiol* (1985). 2001;91(6):2831–2838.
76. Behan M, Zabka AG, Thomas CF, Mitchell GS. Sex steroid hormones and the neural control of breathing. *Respir Physiol Neurobiol*. 2003;136(2–3):249–263.
 77. Dorsey A, de Lecea L, Jennings KJ. Neurobiological and hormonal mechanisms regulating women's sleep. *Front Neurosci*. 2020;14:625397.
 78. Poulsen RC, Warman GR, Sleight J, Ludin NM, Cheeseman JF. How does general anaesthesia affect the circadian clock? *Sleep Med Rev*. 2018;37:35–44.
 79. Luo M, Song B, Zhu J. Sleep disturbances after general anesthesia: current perspectives. *Front Neurol*. 2020;11:629.
 80. Kikuchi T, Tan H, Mihara T, et al. Effects of volatile anesthetics on the circadian rhythms of rat hippocampal acetylcholine release and locomotor activity. *Neuroscience*. 2013;237:151–160.
 81. Liu D, Chen X, Huang Y, et al. Acute continuous nocturnal light exposure decreases BSR under sevoflurane anesthesia in C57BL/6 J mice: possible role of differentially spared light-sensitive pathways under anesthesia. *Am J Transl Res*. 2020;12(6):2843–2859.
 82. Paasonen J, Stenroos P, Salo RA, Kiviniemi V, Grohn O. Functional connectivity under six anesthesia protocols and the awake condition in rat brain. *Neuroimage*. 2018;172:9–20.
 83. Silver NRG, Ward-Flanagan R, Dickson CT. Long-term stability of physiological signals within fluctuations of brain state under urethane anesthesia. *PLoS One*. 2021;16(10):e0258939.
 84. Grahn DA, Heller HC. Activity of most rostral ventromedial medulla neurons reflect EEG/EMG pattern changes. *Am J Physiol*. 1989;257(6 Pt 2):R1496–1505.
 85. Boon JA, Garnett NB, Bentley JM, Milsom WK. Respiratory chemoreflexes and effects of cortical activation state in urethane anesthetized rats. *Respir Physiol Neurobiol*. 2004;140(3):243–256.
 86. Boon JA, Milsom WK. The role of the pontine respiratory complex in the response to intermittent hypoxia. *Respir Physiol Neurobiol*. 2010;171(2):90–100.
 87. Nakamura A, Olson EB, Jr., Terada J, Wenninger JM, Bisgard GE, Mitchell GS. Sleep state dependence of ventilatory long-term facilitation following acute intermittent hypoxia in Lewis rats. *J Appl Physiol* (1985). 2010;109(2):323–331.
 88. Terada J, Mitchell GS. Diaphragm long-term facilitation following acute intermittent hypoxia during wakefulness and sleep. *J Appl Physiol* (1985). 2011;110(5):1299–1310.
 89. Duffy JF, Czeisler CA. Effect of light on Human circadian physiology. *Sleep Med Clin*. 2009;4(2):165–177.
 90. Wever R. [Strength of a light-dark cycle as a time determiner for circadian rhythm in man]. *Pflugers Arch*. 1970;321(2):133–142.
 91. Edmonds SC. Food and light as entrainers of circadian running activity in the rat. *Physiol Behav*. 1977;18(5):915–919.
 92. Neves AR, Albuquerque T, Quintela T, Costa D. Circadian rhythm and disease: relationship, new insights, and future perspectives. *J Cell Physiol*. 2022;237(8):3239–3256.
 93. Jeczmiern-Lazur JS, Orłowska-Feuer P, Smyk MK, Lewandowski MH. Modulation of spontaneous and light-induced activity in the rat dorsal lateral geniculate nucleus by general brain State alterations under urethane anesthesia. *Neuroscience*. 2019;413:279–293.